Early to Late Maastrichtian environmental changes in the Indian Ocean compared with Tethys and South Atlantic

4 authors:

Paula Mateo
California Institute of Technology
15 PUBLICATIONS   38 CITATIONS
SEE PROFILE

Gerta Keller
Princeton University
319 PUBLICATIONS   10,327 CITATIONS
SEE PROFILE

Jahnavi Punekar
Indian Institute of Technology Bombay
17 PUBLICATIONS   129 CITATIONS
SEE PROFILE

Jorge E. Spangenberg
University of Lausanne
246 PUBLICATIONS   2,563 CITATIONS
SEE PROFILE

Some of the authors of this publication are also working on these related projects:

Project   Drinking with the Incas: organic residue analyses of ceramics from Northwest Argentina View project
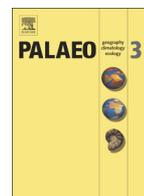
Project   High-resolution correlation in continental-to-marine sections based on δ13C signal View project

Early to Late Maastrichtian environmental changes in the Indian Ocean compared with Tethys and South Atlantic

Paula Mateo [a],[*], Gerta Keller [a], Jahnavi Punekar [b], Jorge E. Spangenberg [c]

[a] Department of Geosciences, Princeton University, Princeton, NJ 08544, USA
[b] Indian Institute of Science Education and Research Pune, Pune 411008, India
[c] Institute of Earth Surface Dynamics, University of Lausanne, Lausanne 1015, Switzerland

ABSTRACT

Planktic foraminiferal analysis, including species populations, diversity trends, high-stress indices and stable isotopes of the latest Campanian through Maastrichtian in the South Atlantic, Tethys and Indian oceans reveal four major climate and faunal events that ended with the Cretaceous-Paleogene (K/Pg), formerly Cretaceous-Tertiary (K/T), mass extinction. The prelude to these events is the late Campanian cooling that reached minimum temperatures in the earliest Maastrichtian (base C31r) correlative with low primary productivity and species diversity. Event-1 begins during the persistent cool climate of the early Maastrichtian (lower C31r) when primary productivity rapidly increased accompanied by rapid species originations, attributed to increased nutrient influx from increased upwelling, erosion during the sea-level fall ~70.6 Ma, and Ninety East Ridge volcanism. During Event-2 (upper C31r to lower C30n), climate rapidly warmed by 2–3 °C in deep waters and peaked at 22 °C on land, primary productivity remained high and diversification reached maximum for the entire Cretaceous. We attribute this climate warming to intense Ninety East Ridge volcanic activity beginning ~69.5 Ma, accompanied by rapid reorganization of intermediate oceanic circulation. Enhanced greenhouse conditions due to the eruption of Deccan Phase-1 in India resulted in detrimental conditions for planktic foraminifera marking the end of diversification. Global cooling resumed in Event-3 (C30n), species diversity declined gradually accompanied by dwarfing, decreased large specialized species, increased small ecologically tolerant taxa, and ocean acidification. Event-3 is mainly the result of enhanced weathering and volcanogenic CO_2 adsorption by the oceans during the preceding warm Event-2 that led to cooling and lower pH in the surface ocean. Event-4 marks the last 250 kyr of the Maastrichtian (C29r), which began with the largest Deccan eruptions (Phase-2) that caused rapid climate warming of 4 °C in deep waters and 8 °C on land, acid rain and ocean acidification leading to a major carbonate crisis preceding the K/T mass extinction.

© 2017 Elsevier B.V. All rights reserved.

1. Introduction

The Maastrichtian (the last stage of the Late Cretaceous, 72.1–66.0 Ma; Gradstein et al., 2012) is a 6.1-Myr time interval that experienced climate and biological extremes ranging from maximum cooling to maximum warming and from maximum marine evolutionary diversity to one of the largest mass extinctions in Earth's history at the Cretaceous/Tertiary (K/T; also known as Cretaceous-Paleogene K/Pg) boundary (review in Keller et al., 2016a).

Despite this remarkable 6.1-Myr history of environmental changes, the Maastrichtian is mostly known for the mass extinction. For the past 30 years, research has concentrated on the K/T boundary centering on a contentious debate: was the mass extinction instantaneous and caused by an asteroid impact or was it more gradual and the result of long-term environmental changes with the asteroid impact the final coup de grace? There are multiple lines of evidence that unquestionably support an impact on the Yucatan Peninsula, Mexico: 1) the global iridium anomaly at the K/T boundary (Alvarez et al., 1980; Alvarez, 1983) that has become the hallmark for all K/T mass extinction studies, 2) discovery of the impact crater on Yucatan (Hildebrand et al., 1991), 3) global distribution of shocked quartz (e.g., Izett, 1990), 4) impact glass spherules discovered throughout the region surrounding the Chicxulub crater (e.g., Smit et al., 1992, Smit et al., 1996; Smit, 1999; Rocchia et al., 1996; Olsson et al., 1997; Norris et al., 1999; MacLeod et al., 2007; Schulte et al., 2010; Keller et al., 2013), and 5) impact breccia in the Chicxulub crater and large breccia and conglomerate deposits lacking impact glass but interpreted as generated by seismic disturbance from the Chicxulub impact (e.g., Bralower et al., 1998; Arenillas et al., 2006; Schulte et al., 2010). Likely environmental consequences of the Chicxulub impact have been widely discussed (e.g., Schultz and

* Corresponding author at: Guyot Hall, Princeton University, Princeton, NJ 08544, USA.
E-mail address: mmateo@princeton.edu (P. Mateo).

D'Hondt, 1996; Tsujita, 2001; Kring, 2007; Vellekoop et al., 2014). This is a formidable list of characteristics that unquestionably identify an impact on Yucatan, but did this impact crash into Yucatan precisely at K/T time and cause the mass extinction as widely inferred? There is stratigraphic, geochemical, sedimentary and fossil evidence that indicates this impact predates the mass extinction by about 100 kyr (Keller, 2014, and references therein). This is a key issue in this ongoing debate over the cause of the K/T mass extinction.

Various advances over the past 10 years have shown that Deccan Trap volcanism in India could have been a critical source of environmental stress leading to the K/T mass extinction: (1) Deccan eruptions were most intense during magnetochron C29r spanning the K/T boundary (Chenet et al., 2007, 2008, 2009); (2) high-precision age based on U-Pb geochronology revealed that 80 % of Deccan eruptions occurred over the ~750 kyr (duration of C29r) with accelerating intensity across the K/T boundary (Schoene et al., 2015); (3) documentation of the mass extinction in intertrappean sediments in India (Keller et al., 2011) between the longest lava flows recorded on Earth (Self et al., 2008); (4) rapid climate warming during C29r below the K/T boundary due to large inputs of volcanogenic greenhouse gases (reviews in Punekar et al., 2014a; Keller et al., 2016a). Based on these studies, it was suggested that the Chicxulub impact might have accelerated Deccan volcanism leading to the mass extinction (Richards et al., 2015; Renne et al., 2015). With this changing perspective, a better understanding of the preceding Maastrichtian environmental changes is imperative and the focus of this study.

One of the first detailed studies on Campanian to early Maastrichtian climate is from Shatsky Rise, Pacific Ocean: stable isotope records based on planktic and benthic foraminifera revealed ~2.5 °C and ~4 °C cooling in surface and bottom waters, respectively (Douglas and Savin, 1975). Subsequent studies on Seymour Island, Antarctica, and ODP Site 690 in the Weddell Sea reported ~2 °C cooling in surface and bottom waters during the early Maastrichtian (Barrera et al., 1987; Barrera and Huber, 1990; Barrera, 1994). The first high-resolution study of Maastrichtian climate and associated faunal turnovers in planktic foraminifera was based on South Atlantic DSDP Site 525A (Li and Keller, 1998a, 1998b; Abramovich and Keller, 2003). These studies revealed that the generally cool Maastrichtian climate was interrupted by two rapid warm events: 1) at the early to late Maastrichtian transition (also known as mid-Maastrichtian event) with a 2–3 °C warming of surface and bottom waters, and 2) in the latest Maastrichtian below the K/T boundary (C29r) when surface and bottom waters warmed rapidly by 4 °C. An updated high-resolution stable isotope record for the late Campanian to early Maastrichtan at Site 525A confirmed the observed cooling and warming events (Friedrich et al., 2009). Since Li and Keller (1998a, 1998b), the latest Maastrichtian C29r rapid marine warming has been documented globally (e.g., Barrera and Savin, 1999; MacLeod et al., 2005; Isaza-Londoño et al., 2006; Tobin et al., 2012; Thibault and Husson, 2016) and recently linked to the main phase of Deccan volcanism (reviews in Punekar et al., 2014a; Keller et al., 2016a). Some studies correlate the Maastrichtian terrestrial and marine climate records demonstrating that the same extreme climate changes occurred also on land (Nordt et al., 2003; Wilf et al., 2003).

In addition to the climate record, various studies focused on Maastrichtian primary productivity, sea-level fluctuations and the marine biotic response to climate changes based on planktic foraminifera (e.g., Li and Keller, 1998a, 1998c; Zepeda, 1998; Premoli Silva and Sliter, 1999; Li et al., 2000; MacLeod et al., 2001; Olsson et al., 2001; Abramovich and Keller, 2002, 2003; Abramovich et al., 2003, 2010; Hart, 2007; Punekar et al., 2014b) and nannofossils (e.g., Eshet and Almogi-Labin, 1996; Friedrich et al., 2005; Thibault and Gardin, 2007, 2010; Gardin et al., 2012; Thibault, 2016; Thibault and Husson, 2016). A particular focus of these studies is the early to late Maastrichtian warming and associated minor extinctions (review in Keller et al., 2016a) as well as the rapid warming during C29r and associated diversity decline (review in Punekar et al., 2014a).

The eruption of Large Igneous Provinces (LIPs) have been shown to be a direct cause for climate change (both cooling and warming), acid rains, ocean acidification and large inputs of toxic metals, as well as an indirect cause for anoxia and changes in sea-level and oceanic circulation disruptions, leading to major faunal turnovers including mass extinctions (e.g., Siberian Traps and Permo-Triassic, Central Atlantic (CAMP) and the Triassic-Jurassic, Deccan Traps and Cretaceous-Tertiary) (Wignall, 2001; Courtillot and Renne, 2003; Bond and Wignall, 2014; Courtillot and Fluteau, 2014). During the Maastrichtian, Ninety East Ridge volcanism in the Indian Ocean was active (e.g., Duncan, 1978, 1991; Pringle et al., 2008; Krishna et al., 2012) and overlapped the eruption of Deccan phase-1 in India (Chenet et al., 2009; Schöbel et al., 2014) potentially contributing to the climate and faunal changes recorded during this time.

The main objective of this study is to evaluate the environmental effects of climate change and major volcanic eruptions on marine planktic foraminifer diversity during the Maastrichtian. We test the hypothesis that volcanism was the main driver of the evolutionary diversification in the early Maastrichtian, the likely cause for the early to late Maastrichtian climate warming, and the latest Maastrichtian warming (C29r) and high-stress environments. We focus on five localities from the Indian Ocean (Ninety East Ridge Site 217, Cauvery Basin, SE India), Tethys (El Kef and Elles, Tunisia) and South Atlantic (Site 525A) (Fig. 1). Analyses concentrate on: 1) high-resolution quantitative analysis of planktic foraminifera to determine biostratigraphy and assess the timing and nature of faunal turnovers at Site 217; 2) update taxonomy of the Tethys and South Atlantic sites, and extend the Cauvery Basin record through the early Maastrichtian to compare diversity trends through the Maastrichtian; 3) oxygen and carbon stable isotopes of planktic and benthic foraminifera at Site 217 to evaluate changes in climate and productivity compared with Site 525A; 4) planktic foraminiferal indices, including diversity, dwarfing, planktic/benthic ratio and fragmentation index, to gain a deeper understanding of the changing environment and associated faunal responses; and 5) correlation of sedimentation records, hiatus distribution and sea-level changes across regions Indian, Tethys and South Atlantic oceans to understand regional and global effects of climate and ocean circulation changes.

2. Materials and Methods

DSDP Site 217 (8°55.57″N, 90°32.33′E) is located in the Indian Ocean on the northernmost part of the Ninety East Ridge at a water depth of 3010 m (Von der Borch et al., 1974). Ninety East Ridge is interpreted as a volcanic chain formed by the northward migration of the Indian plate over the Kerguelen mantle plume that was active from the late Cretaceous to the Paleogene (e.g., Duncan, 1978, 1991; Pringle et al., 2008; Krishna et al., 2012). With the passage over the mantle plume, lithospheric uplift led to the formation of volcanic islands and the deposition of thick ash sequences and shallow water sediments overlying the basement (Moore et al., 1974; Thompson et al., 1974; Coffin, 1992); passage beyond the mantle plume led to rapid subsidence as the oceanic lithosphere cooled (Sclater and Fisher, 1974; Luyendyk, 1977; Coffin, 1992). Based on a linear progression rate of 118 km/Myr, an age of ~80 Ma was estimated for the location of Site 217 at the time of its position over the mantle plume (Pringle et al., 2008), which is consistent with the Campanian age of the oldest sediments recovered with shallow water affinities overlying the basement (Von der Borch et al., 1974). A progressive deepening to a depth of ~1000 m is recorded during the early to late Maastrichtian as indicated by the transition to foraminifera-rich nannofossil ooze (Von der Borch et al., 1974; Tantawy et al., 2009).

Samples were taken every ~50 cm from cores 17 to 21; planktic foraminifera were originally analyzed by Alfonso Pardo and published in Tantawy et al. (2009). For this study, the species identifications were updated and additional size fractions were analyzed to focus on the very small (38–63 μm), small (63–150 μm) and larger (>150 μm) size
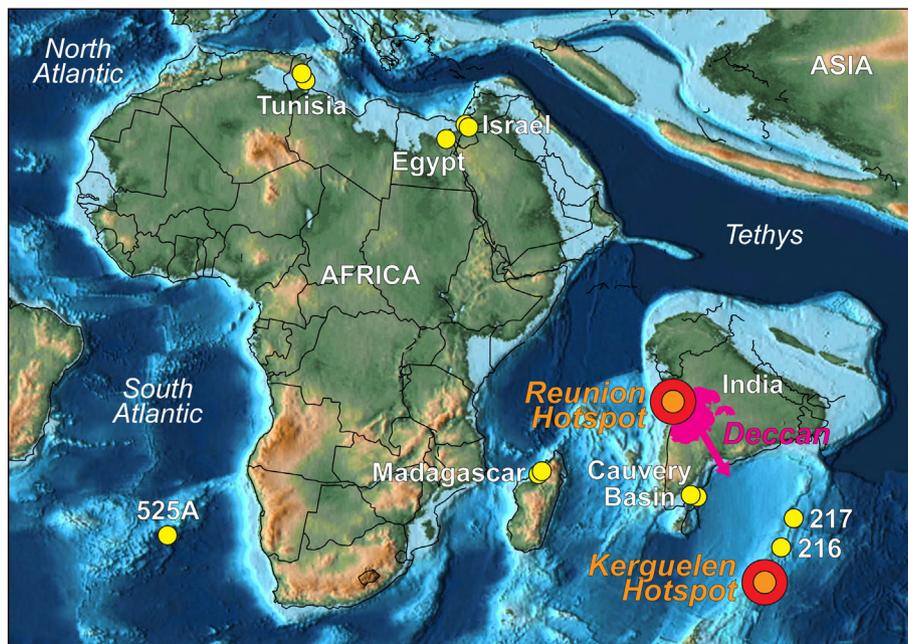
Fig. 1. Paleolocation (66 Ma) of Maastrichtian sections, Reunion and Kerguelen hotspots and Deccan volcanism discussed in this study. Paleomap from Scotese (2013).

fractions as environmental indicators. In addition, sample resolution was increased and additional samples were added to extend the record through core 23. A total of 70 samples were analyzed.

For paleontological analyses, samples were processed in the laboratory following the procedure described by Keller et al. (2002). Samples were soaked overnight in 3 % hydrogen peroxide solution to oxidize organic carbon. After disaggregation of sediment particles, the samples were washed through >63 μm and >38 μm sieves to obtain clean foraminiferal residues. Washed residues were oven dried at 50 °C. Quantitative planktic species analyses were performed based on aliquots of 300 specimens in the 38–63 μm, 63–150 μm and >150 μm size fractions, with the remaining residues in each sample fraction examined for rare species. All specimens were identified based on standard taxonomic concepts (Robaszynski et al., 1983-1984; Nederbragt, 1991) and mounted on microslides for a permanent record.

Oxygen and carbon isotope analyses were performed on monospecific benthic foraminiferal tests (*Gavelinella beccariformis* and *Cibicidoides* species) in laboratories at Karlsruhe University, Germany, and at the University of Lausanne, Switzerland. At the Karlsruhe laboratory, the data were obtained using a fully automated preparation system (MultiCarb) connected on-line to an isotope ratio mass spectrometer (Optima, Micromass Limited UK). All carbon and oxygen isotope values are reported relative to the VPDB standard, with reproducibility better than 0.1 ‰ (2σ). At the UNIL laboratory, analyses were performed for cores 21–23 with a Thermo Fisher Scientific (Bremen, Germany) GasBench II connected to a Thermo Fisher Scientific Delta Plus XL IRMS, in continuous He-flow mode. Analytical uncertainty (2σ) monitored by replicate analyses of the international calcite standard NBS-19 ($\delta^{13}C = +1.95$ ‰, $\delta^{18}O = -2.20$ ‰) and the laboratory standard Carrara Marble ($\delta^{13}C = +2.05$ ‰, $\delta^{18}O = -1.70$ ‰) was better than ±0.05 ‰ for $\delta^{13}C$ and ±0.1 ‰ for $\delta^{18}O$. Results from both laboratories are comparable based on replicate analyses.

Species diversity was estimated based on cumulative species richness: number of species theoretically present in any given sample from first evolutionary appearance to extinction, ignoring any temporary exclusion (Abramovich and Keller, 2002). Species dwarfing estimates were based on the number of 150–250 μm specimens in the >150 μm size fraction of each sample. The planktic/benthic foraminiferal ratio was based on the number of benthic foraminifera associated

with the aliquot of 300 planktic foraminifera used for the quantitative species analysis in the 63–150 μm size fraction.

The fragmentation index (FM) was analyzed based on aliquots of approximately 500–700 foraminifera and fragments in the >63 μm size fraction. Three categories were identified based on the quality of preservation: 1) nearly perfect tests (good), 2) partially damaged, imperfect tests with holes (fair), and 3) fragments, less than two-thirds of an entire test (poor) (Punekar et al., 2016). The FM index was calculated as *fragments* % = (*fragments*/8)/[(*fragments*/8) + *whole tests*] (Williams et al., 1985; Malmgren, 1987). Based on the assumption that each test breaks into an average of 8 fragments, the equation requires the total number of counted fragments to be divided by 8 to estimate the original number of whole tests.

At the Cauvery Basin, India, we chose the Kali-H subsurface core previously analyzed in Keller et al. (2016b) for the upper Maastrichtian and extended this record through the lower Maastrichtian concentrating on species diversity and ranges from first to last appearances. To insure that the same species concepts were used in faunal analyses, species identifications were updated for the Tunisian sections in Elles and El Kef (Li and Keller, 1998c; Abramovich and Keller, 2002) and South Atlantic DSDP Site 525A (Li and Keller, 1998a).

3. Biostratigraphy

3.1. Ninety East Ridge DSDP Site 217, Indian Ocean

High-resolution planktic foraminiferal biostratigraphy is a powerful tool for relative age dating and to assess the continuity of sediment deposition. In this study, we apply the Cretaceous foraminiferal (CF) biozonation of Li and Keller (1998a) and correlate the results with localities from the Indian, Tethys and South Atlantic oceans (Fig. 2).

The Maastrichtian interval at DSDP Site 217 spans zones CF8 to CF2 and was analyzed in two size fractions, >150 μm to evaluate relative abundances of larger specialized species and 63–150 μm to evaluate the smaller ecological generalist taxa.

Zone CF8 is defined by the first appearance (FA) of *Globotruncana aegyptiaca* at the base and the FA of *Gansserina gansseri* at the top (Fig. 2). At Site 217, a 5 m core gap prevents full assessment of zone CF8 and only the upper part may be present, assuming that the first
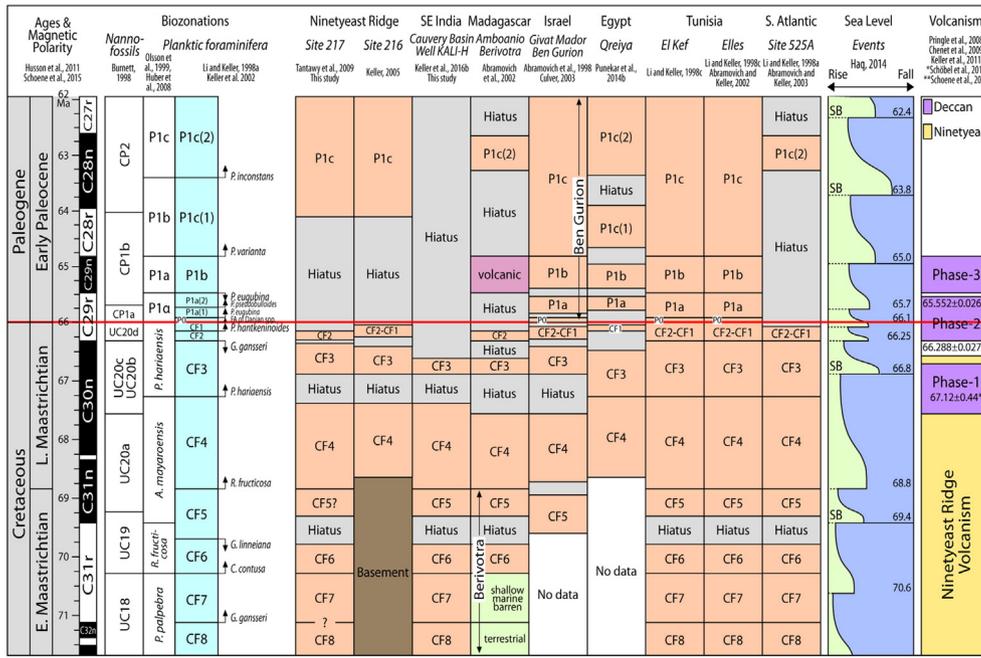
Fig. 2. Maastrichtian-early Paleocene biostratigraphy for planktic foraminifera is based on the zonation scheme of Keller et al. (2002) and Li and Keller (1998a) and plotted against the magnetic polarity time scale of Site 525A (Husson et al., 2011). Other zonal schemes are shown for comparison (Burnett, 1998; Olsson et al., 1999; Huber et al., 2008). Note the overall correlation of hiatuses (Abramovich et al., 1998, 2002; Li and Keller, 1998c; Abramovich and Keller, 2002, 2003; Culver, 2003; Keller, 2005; Tantawy et al., 2009; Punekar et al., 2014b; Keller et al., 2016b) and sea-level events (Haq, 2014), particularly the increased number of erosion events beginning in C30n, correlative with the onset of Deccan volcanism, reflecting increased climate variability, intensified currents and erosion.

appearance of *G. aegyptiaca* occurs below the analyzed interval (Fig. 3). Nine species appear above the core gap based on both size fractions (>150 μm, 63–150 μm). These species originations are part of the gradual diversification event that began in zone CF8 and was previously observed at Elles and El Kef, Tunisia, and South Atlantic DSDP Site 525A (Li and Keller, 1998a, 1998c).

Zone CF7 spans the interval between the FA of *G. gansseri* at the base and the FA of *Contusotruncana contusa* at the top (Fig. 2). At Site 217, a gradual increase in the relative abundance of *Gublerina rajagopalani* from 6.5 % to 16 % is observed in the >150 μm size fraction (Fig. 3) and in *Heterohelix planata* from 23 % to 45 % in the 63–150 μm size fraction (Fig. 4). These species have been shown to tolerate and thrive in a
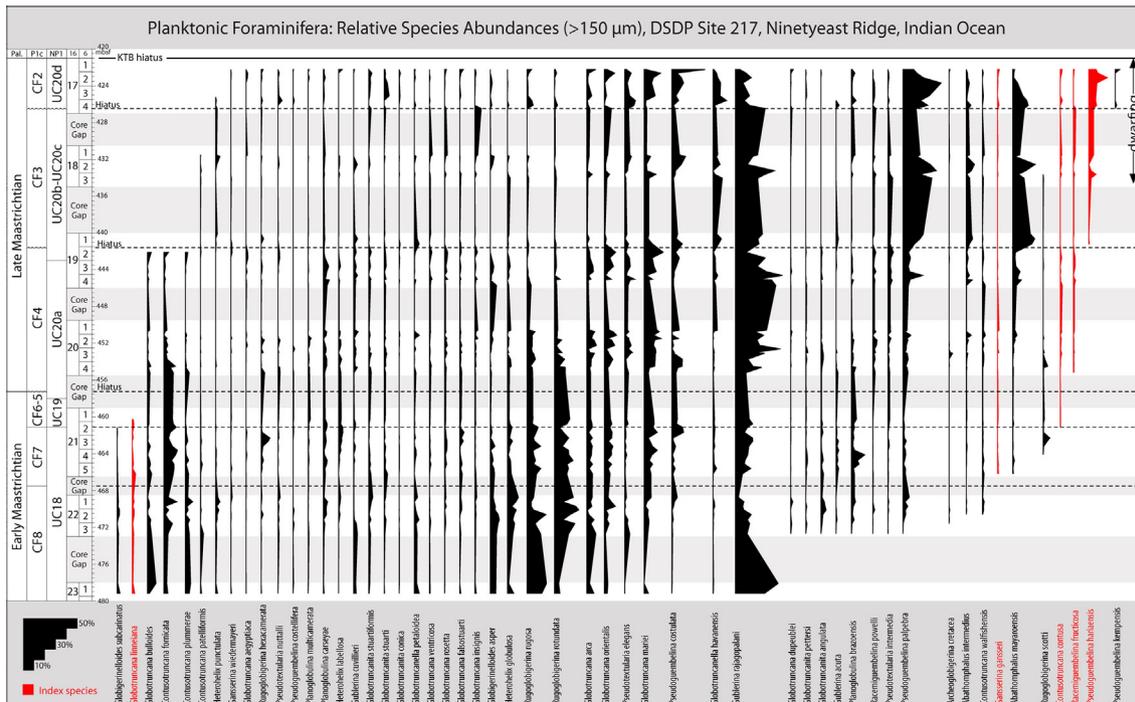

Fig. 3. Maastrichtian biostratigraphy and relative species abundances of planktic foraminifera (>150 μm size fraction) at Ninety East Ridge DSDP Site 217, Indian Ocean.
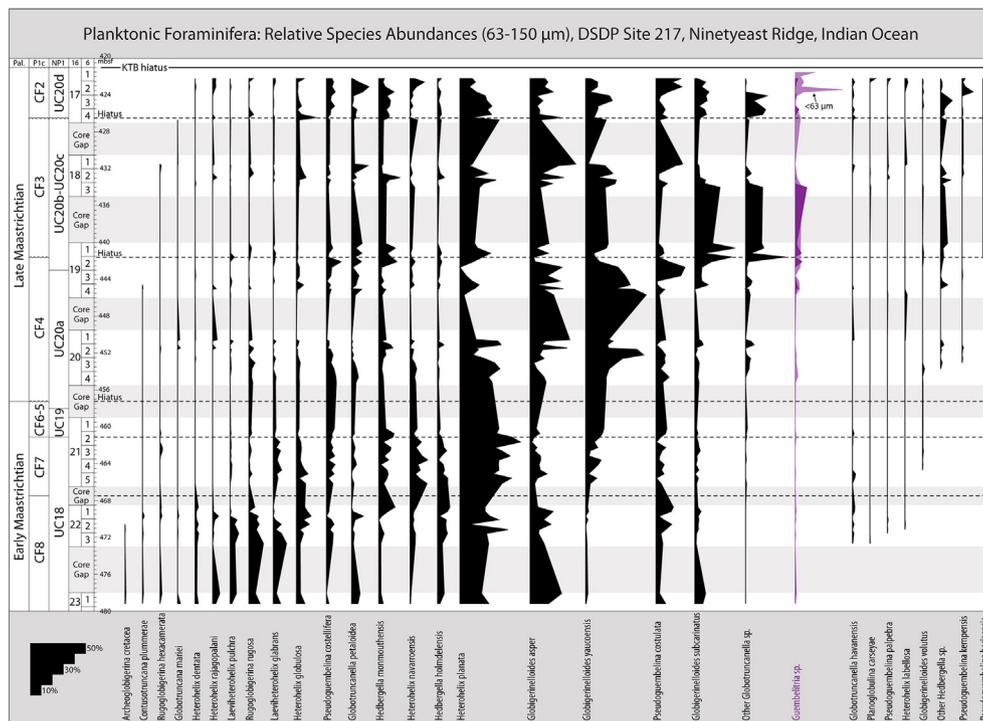
Fig. 4. Maastrichtian biostratigraphy and relative species abundances of planktic foraminifera (63–150 μm size fraction) at Ninety East Ridge DSDP Site 217, Indian Ocean. Note increased abundance of *Guembelitria cretacea* in zone CF3 (dark purple) and abundance peaks in the 38–63 μm size fraction (light purple), indicating increasingly high-stress environments in zone CF3. (For interpretation of the references to colour in this figure legend, the reader is referred to the web version of this article.)

wide range of environmental conditions (i.e., dominant in high-stress environments affected by temperature, salinity, nutrients and oxygen variations in which large specialized species struggle to survive), thus their increasing population abundances suggest increasing stressed environments (e.g., Pardo and Keller, 2008; Keller and Abramovich, 2009).

Zone CF6 is defined by the FA of *C. contusa* at the base and the last appearance (LA) of *Globotruncana linneiana* at the top. The latter species also marks the base of zone CF5 and the FA of *Racemiguembelina fructicosa* defines the top (Fig. 2). At Site 217, zone CF6 is at least partially present, but zone CF5 is not recognized due to a core gap and likely hiatus as just ~2 m of sediments represent the combined CF6–CF5 interval (Figs. 3, 4). In contrast, these two zones span 8 m and 5 m in the Cauvery Basin of SE India (Keller et al., 2016b), 6.5 m and 9.5 m at South Atlantic Site 525A, (Li and Keller, 1998a), 4 m and 13 m at El Kef, and 4.5 m and 6.5 m at Elles, Tunisia (Li and Keller, 1998c), respectively. However, at Site 525A and the Tunisian sections, zone CF6 is condensed (~5 m) suggesting widespread erosion between CF5 and CF6, coincident with a sea-level fall and major sequence boundary (SB) dated at 69.4 Ma (Fig. 2) (Haq et al., 1987; Haq, 2014).

Zone CF4 spans the interval from the FA of *R. fructicosa* at the base to the FA of *Pseudoguembelina hariaensis* at the top (Fig. 2). At Site 217, a minor extinction event is marked by the disappearances of *Contusotruncana fornicata*, *C. plummerae* and *Globotruncana bulloides* (Fig. 3). These species disappearances, frequently including *Archeoglobigerina cretacea*, have also been recognized at Site 525A, Madagascar, Israel, Egypt, Tunisia, Poland and SE India (Li and Keller, 1998a, 1998c; Abramovich et al., 1998, 2002, 2010; Dubicka and Peryt, 2012; Meilijson et al., 2014; Punekar et al., 2014b; Keller et al., 2016b). Zone CF4 is marked by decreased abundance of *Rugoglobigerina rotundata* from 10 % to 3 % and *R. rugosa* from 5 % to 2 %, and increased abundance of *G. rajagopalani* from 10 % to 43.5 % followed by a rapid decrease to 20 % towards the top of CF4 (Fig. 3). In the smaller size fraction (63–150 μm), major species variations include decreased abundance of *H. planata* parallel to increased abundances of *Globigerinelloides yaucoensis*

from 19 % to 54.5 % and *G. asper* from 14 % to 36 %, reaching minimum values at the CF4/CF3 boundary (Fig. 4).

The CF4/CF3 boundary is marked by a hiatus as suggested by the abrupt decrease in all larger (>150 μm) species abundances (Fig. 3) and increase in very small stress-tolerant species (e.g., globigerinelloides, globotruncanellids, hedbergellids, guembelitrids, Fig. 4). A hiatus at the CF4/CF3 transition coincides with a major sea-level fall and SB ~66.8 Ma (Haq et al., 1987; Haq, 2014) and is recorded worldwide (e.g., SE India, Keller et al., 2016b; Madagascar, Abramovich et al., 2002; Israel, Abramovich et al., 1998; Fig. 2).

Zone CF3 is defined by the FA of *P. hariaensis* at the base and the LA of *G. gansseri* at the top (Fig. 2). At Site 217, *G. rajagopalani* and *Pseudoguembelina palpebra* dominate and *Abathomphalus mayaroensis* is common in the >150 μm size fraction of zone CF3 assemblages (Fig 3). Dwarfed specimens are common in several horizons (424.08 m, 424.59 m, 425.19 m, 426.70 m, 432.96 m, and 441.58 m). In the smaller size fraction (63–150 μm) *Heterohelix*, *Globigerinelloides,* and *Globotruncanella* (*havanensis, petaloidea*) species dominate (Fig. 4). The disaster opportunist *Guembelitria cretacea* records increased abundances from 1 % to 5 % on average. These faunal changes indicate continued and even increasing high-stress environments during zone CF3 compared with zone CF4 (e.g., Pardo and Keller, 2008; Keller and Abramovich, 2009).

The CF3/CF2 transition is represented by a hiatus marked by abrupt changes in the relative abundances of larger species (Fig. 3) and smaller species (Fig. 4). This hiatus coincides with a sea-level fall ~66.25 Ma (Haq et al., 1987; Haq, 2014) and is commonly observed in the Indian and Tethys Oceans (e.g., Abramovich et al., 1998, 2002; Keller, 2005; Tantawy et al., 2009; Punekar et al., 2014b; Fig. 2).

Zone CF2 spans the interval from the LA of *G. gansseri* at the base to the FA of *Plummerita hantkeninoides* at the top (Fig. 2). At Site 217, this zone is marked by decreased abundance of *Gublerina rajagopalani* from 27 % to 10 % and increased *Pseudoguembelina palpebra* from 12 % to 20 % in the >150 μm size fraction (Fig. 3). In the 63–150 μm size fraction,

small species abruptly increase (e.g., *Heterohelix, Globigerinella, Globotruncanella, Hedbergella*). *Pseudoguembelina costulata*, a surface dweller, dominates both the larger and the smaller size fractions towards the top of the section, with peak abundances of 31 % and 20 %, respectively. This change is accompanied by a rapid increase in the abundance of *Guembelitria* species in the 38–63 μm size fraction suggesting severe high-stress environments just before the KTB hiatus (Fig. 4).

At Site 217, a major hiatus (~2 Myr) spans from the upper part of zone CF2 through the latest Maastrichtian zone CF1 and early Danian zones P0, P1a, P1b and lower P1c (Fig. 2). On a global basis, erosion is less extensive in this interval but marked by repeated short hiatuses. This erosion pattern is commonly attributed to rapid climate changes, periods of global cooling, intensified bottom-water circulation, and sea-level fluctuations across the K/T transition (e.g., MacLeod and Keller, 1991; Keller et al., 2013; Mateo et al., 2016).

3.2. Correlation: Indian, Tethys and South Atlantic oceans

Biostratigraphic correlation of localities across the Indian, Tethys and South Atlantic oceans compared with major sea-level changes and volcanic eruptions in India (Deccan Traps) and Ninety East Ridge reveal similarities and differences in sedimentation related to these events (Fig. 2). Although the current study concentrates on the Maastrichtian, the early Paleocene (Danian) record is also shown as it illustrates the pivotal change in sediment deposition and erosion pattern that began in the late Maastrichtian zone CF3.

The early Maastrichtian sediment record across the regions is remarkably continuous despite major sea-level fluctuations, Ninety East Ridge volcanic eruptions and associated climate changes (Fig. 2). The only significant interruption coincides with the sea-level fall and sequence boundary (SB) at ~69.4 Ma (Haq, 2014) correlative with zone CF5. The likely reasons for the reduced sediment erosion include lower magnitude of sea-level changes, overall higher Cretaceous oceans inundating continents, higher rate of carbonate sedimentation and relatively low levels of volcanic eruptions.

In contrast, sedimentation is highly fragmented during the latest Maastrichtian beginning in zone CF3 and continuing through the early Danian, except for areas protected from erosion, particularly in Tunisia (Fig. 2). Sediment erosion (hiatus) generally coincides with sea-level changes in zones CF4/CF3, CF3/CF2, KTB, P1a/P1b, P1b/P1c and P1c/P2. On Ninety East Ridge, Southeast India (Cauvery Basin), Madagascar and South Atlantic, erosion removed sediments spanning most of the early Danian and frequently through the KTB and zones CF1–CF2. This massive erosion is also observed in the North Atlantic (Keller et al., 2013; Mateo et al., 2016) and appears related to the significant sea-level fall at ~63.8 Ma, but a series of smaller sea-level falls contributed to erosion that resulted in shorter hiatuses observed in the Tethys (e.g., Israel, Egypt) and many deep-sea sections. However, the major erosion observed during the latest Maastrichtian through Danian can be attributed to the overall cooler climate (except for the short warming in C29r), lower sea-level and higher frequency of sea-level falls beginning in CF3 (C30n).

4. Stable isotopes: Productivity and temperature changes

Carbon and oxygen isotopes of the benthic foraminifera *Gavelinella beccariformis* were analyzed for the Maastrichtian at Site 217, except for zone CF8 where this species is rare and *Cibicidoides* species were analyzed instead. Both of these species are commonly used to evaluate deep-water changes in productivity and temperature (e.g., Shackleton, 1987; Zachos et al., 1989; Schrag et al., 1995; D'Hondt and Arthur, 2002). Although Site 217 has a fragmented record because of frequent core gaps, $\delta^{13}C$ and $\delta^{18}O$ trends are similar to Site 525A (Li and Keller, 1998a), except for zones CF8–CF7. At Site 217, $\delta^{13}C$ values are significantly higher in CF8 (+1.46 ‰) and fluctuating in CF7 (+0.90 to +1.93 ‰) compared to Site 525A (+0.33 ‰ and +0.50 to +1.17 ‰, respectively) (Fig. 5). At Site 525A, $\delta^{13}C$ values record an increase of +1.5 ‰ through the early Maastrichtian that is not observed at Site 217 (Fig. 5). This difference likely reflects higher, more stable primary productivity at Site 217 due to higher nutrient inputs from Ninety East Ridge volcanism that began ~82 Ma (Coffin et al., 2002). Species effects are
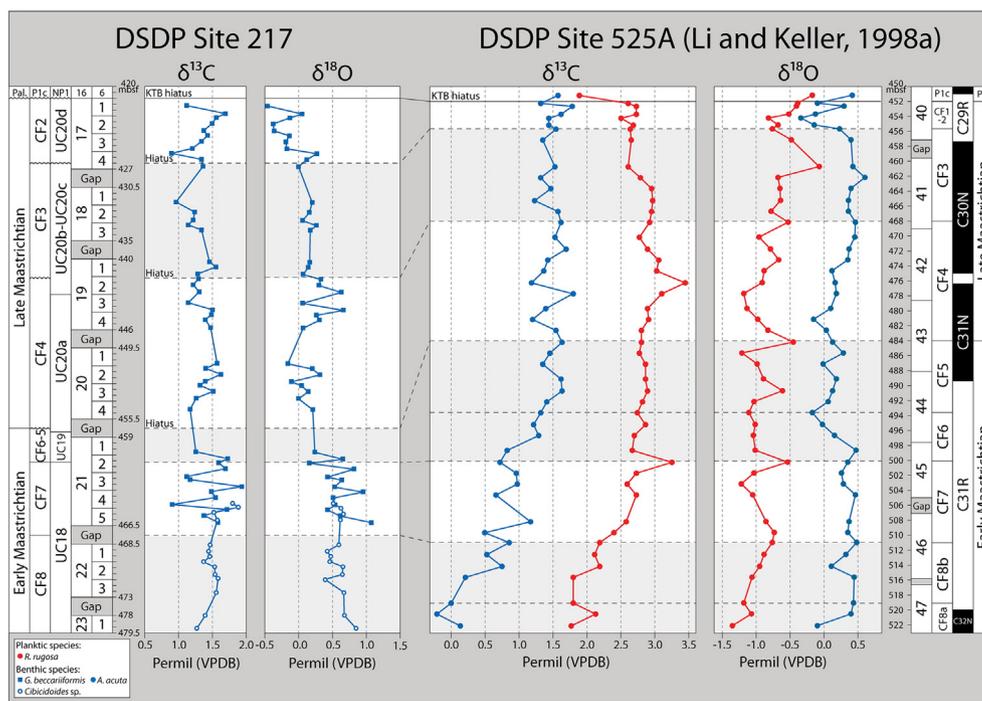
Fig. 5. Maastrichtian stable isotopic data of benthic foraminifera (*Gavelinella beccariformis* and *Cibicidoides* species) recording climate and productivity changes in bottom waters at Ninety East Ridge DSDP Site 217, Indian Ocean, as compared with South Atlantic DSDP Site 525A (Li and Keller, 1998a). Note the warm-cool transition in CF4 (from low to high δ18O values). The low-resolution record at Site 525A (Li and Keller, 1998a) is consistent with high-resolution records by Li and Keller (1998b) and Friedrich et al. (2009).

another potential contributing factor to this difference because *G. beccariformis* at Site 217 is compared with *Anomalinoides acuta* at Site 525A (e.g., Friedrich et al., 2006).

At Site 217, the CF6–CF5 interval is incomplete due to a core gap and possibly a hiatus. In zone CF4, $\delta^{13}C$ values range from +1.1 ‰ to +1.6 ‰ similar to Site 525A (+1.2 ‰ to +1.7 ‰), suggesting sustained high primary productivity at both sites (Fig. 5). $\delta^{18}O$ values increase from +0.1 ‰ to +0.7 ‰ towards the top of zone CF4 at Site 217 marking cooling also comparable to Site 525A where $\delta^{18}O$ values increase from +0.1 ‰ to +0.5 ‰ (Fig. 5). In zones CF3–CF2, Site 217 $\delta^{13}C$ values vary from +0.9 ‰ to +1.7 ‰ similar to Site 525A (+1.2 to +1.8 ‰); in zone CF2, Site 217 $\delta^{18}O$ values decrease from +0.3 ‰ to −0.5 ‰, also comparable to Site 525A (+0.4 ‰ to −0.3 ‰), indicating climate warming.
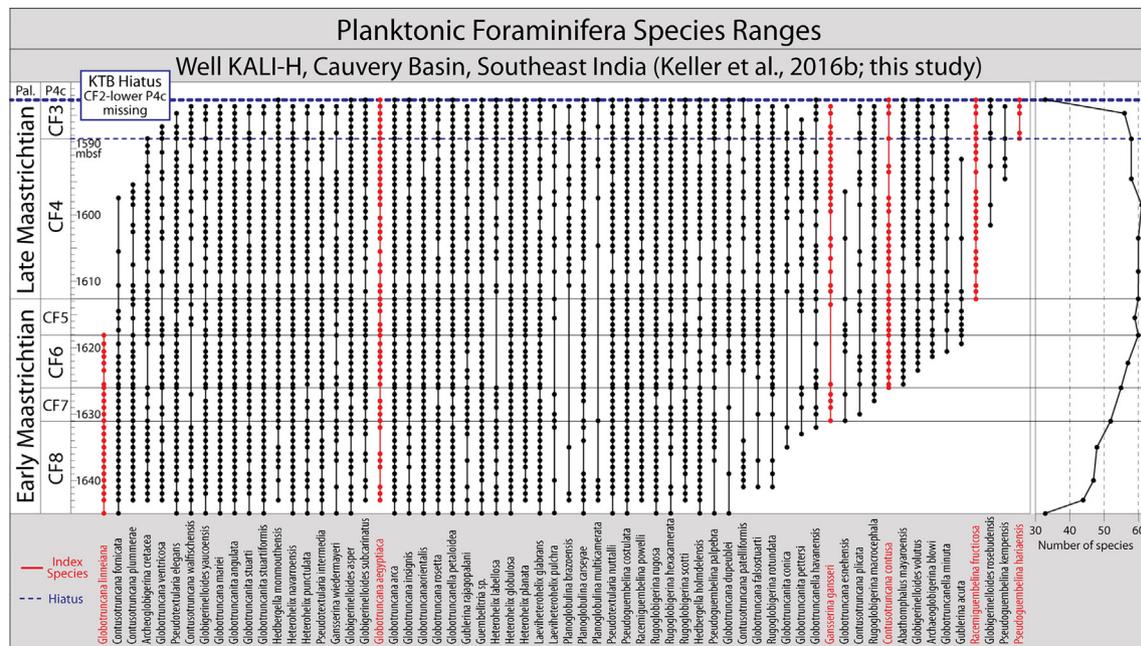
5. Diversity trends

Planktic foraminifera are characterized by major evolutionary diversification in the early Maastrichtian and the mass extinction at the K/T boundary (review in Li and Keller, 1998a). The cause for this diversification event has remained an enigma and its potential contribution to the mass extinction is rarely considered. We use species ranges and cumulative species richness in the Indian, Tethys and South Atlantic oceans to investigate the early Maastrichtian origination event and the fate of the new species leading up to the mass extinction. In the Indian Ocean Ninety East Ridge Site 217 (Fig. 6) and the Kali-H well from the Cauvery Basin, SE India (Fig. 7), sediment deposition and faunal changes occurred at depths of 500–1000 m (upper to middle bathyal; Von der Borch et al., 1974; Tantawy et al., 2009) and 300–500 m (outer shelf to upper bathyal; Keller et al., 2016b), respectively. The El Kef and Elles sections in Tunisia (Fig. 8) were deposited in outer shelf to upper slope (300–500 m) and middle to outer shelf (200–300 m) depths, respectively. These are the two most complete Maastrichtian sedimentary records known worldwide (Fig. 2) (Li and Keller, 1998c; Abramovich and Keller, 2002). In the South Atlantic, Site 525A (Fig. 9) sediment deposition during the Maastrichtian occurred in a middle bathyal

environment (~1000 m) (Li and Keller, 1998a). The paleodepth of these five localities thus yield comparable marine settings spanning open-ocean to continental shelf environments that permit assessment of species diversity, population abundances and faunal turnovers. Census data are summarized in Table 1 as cumulative species diversity per biozone.

5.1. Diversity maximum: Early Maastrichtian

In the Indian Ocean, the early Maastrichtian zones CF8–CF5 reveal 14 species originations at Site 217 (Fig. 6) and 16 species originations at the Cauvery Basin well Kali-H (Fig. 7). Note that in these sections only part of zone CF8 is present but the number of species originations not yet reached at these sites can still be estimated based on Tunisia and Site 525A. At El Kef, 21 species originations occurred in the early Maastrichtian, which is comparable to Elles with 18 species (Fig. 8). At Site 525A, 23 species originations are identified during this interval (Fig. 9). Most of these species are also present in the Indian Ocean Site 217 and Kali-H but the first appearances of some are not recorded because of incomplete core recovery. If we add those first appearances, then species originations at Site 217 and Kali-H increase to 22 and 25 species, respectively (Table 1). Elles and Site 525A also show 7 and 6 species originations in zones CF9–CF8b, indicating gradual diversification already beginning in the latest Campanian.

Most of the species originations occurred among subsurface and thermocline dwellers. The latter probably originated as subsurface dwellers that later migrated to thermocline depths during warm intervals and increased water mass stratification (Abramovich et al., 2003). Originations are likely due to a major increase in nutrient availability driving primary productivity (Fig. 5) and faunal diversification (Hallock, 1987). Ninety East Ridge volcanism was probably a major contributor of nutrients in the Indian Ocean as suggested by the inferred total number of species originations (22 at Site 217, 25 at Kali-H; Table 1) although recovery is incomplete for the base CF8–CF9 interval (Figs. 6, 7). Maximum diversity is reached during the CF6/CF5 transition in Kali-H and Elles, and in the lower part of zone CF4 at Sites 217 and

Fig. 6. Biostratigraphy of Maastrichtian planktic foraminifera at Ninety East Ridge DSDP Site 217, Indian Ocean. Species ranges based on composite occurrences in the >150 μm and 63–150 μm size fractions. Index species marked in red. Note rapid species originations in zones CF8–CF6 and a minor extinction event in zone CF4. (For interpretation of the references to colour in this figure legend, the reader is referred to the web version of this article.)

Fig. 7. Biostratigraphy of Maastrichtian planktic foraminifera in Kali-H well, Cauvery Basin, India (Keller et al., 2016b; this study). Index species marked in red. Note rapid species originations in zones CF8–CF6 and a minor extinction event in zone CF4. (For interpretation of the references to colour in this figure legend, the reader is referred to the web version of this article.)

525A. At El Kef, the diversity maximum is at the base of CF3, but the late Maastrichtian record is suspect because of major faults in the area that complicate stratigraphy (Li and Keller, 1998c).

5.2. Minor extinction event: Early to Late Maastrichtian

A minor extinction event coincides with the end of climate warming in the early late Maastrichtian and is commonly known as "mid-Maastrichtian event" (e.g., MacLeod, 1994; Barrera and Savin, 1999; Li and Keller, 1998a, 1999; Nordt et al., 2003; Frank et al., 2005; Friedrich et al., 2009; Keller et al., 2016a; Thibault, 2016). This mid-Maastrichtian event is also observed in all sections analyzed for this study.

At Site 217, this minor extinction event is observed at the CF4/CF3 transition and marked by the disappearances of *Contusotruncana fornicata*, *C. plummerae* and *Globotruncana bulloides,* with *Archeoglobigerina cretacea* and *Gublerina acuta* disappearing in zone CF3 above the CF4/CF3 hiatus (Fig. 6). In the Cauvery Basin Kali-H well, this event also includes the disappearances of *C. fornicata*, *C. plummerae,* as well as *A. cretacea, G. acuta* and *Globotruncana esnehensis*. Because the latter two species are known to range higher in the stratigraphic record (e.g., Li and Keller, 1998a; Abramovich and Keller, 2002; Abramovich et al., 2002; Darvishzad et al., 2007; Huber et al., 2008; Punekar et al., 2014b), their early disappearance in the Indian Ocean suggests regional differences (e.g., diachronous occurrences) in species ranges.

At El Kef and Elles, the disappearances of *C. fornicata* and *C. plummerae* occur in zone CF5, rather than CF4 (Fig. 8). At El Kef, this may be due to the incomplete Maastrichtian record cut by major faults, but at Elles the late Maastrichtian is undisturbed, suggesting that the zone CF4 index species *R. fructicosa* may be diachronous in the shallower middle shelf environment, or that high-stress conditions were more severe in shallower environments (e.g., Leckie, 1987). At Site 525A, *C. fornicata*, *G. bulloides*, *C. plummerae*, *A. cretacea* and *Globotruncana ventricosa* gradually disappear in zone CF4 (Fig. 9). This minor extinction event has also been recorded in Madagascar, Israel, Egypt and Poland (Abramovich et al., 2002, 2010; Dubicka and Peryt, 2012; Punekar et al., 2014b; Keller et al., 2016a). From shallow to deep environments, this faunal turnover seems to have been the result of global environmental perturbations that coincide with the transition from warm to cool climate (Fig. 5) associated with reduced water mass stratification, increased competition and biotic stress leading to the extinction of specialized subsurface and thermocline dwelling species.

5.3. Late Maastrichtian diversity decline preceding the mass extinction

A major faunal turnover in species populations, but minor change in species diversity, is generally observed in zone CF3 (Figs. 6–8) correlative with maximum cooling, suggesting increased stress conditions as evident by the decreased relative abundances of specialist species and increased abundance of generalist species more tolerant of environmental changes (further discussed in Section 6.1). In zones CF2–CF1, diversity gradually decreased along with further reduction in specialist species populations prior to the very rapid mass extinction at the K/T boundary (Figs. 8, 9). Environmental changes in zones CF2–CF1 have been widely studied and recently linked to the massive Deccan eruptions and volcanic degassing that led to climate warming, eutrophication and ocean acidification contributing to this major biotic crisis (e.g., Punekar et al., 2014a, 2016; Font et al., 2014, 2016; Thibault, 2016).

6. Environmental effects

6.1. Ecological associations and depth ranking

Planktic foraminiferal assemblages consist of three main ecological groups: specialists, generalists and disaster opportunists. Specialists species, known as K-strategists, are diverse species with large, complex tests, that tolerate a narrow range of environmental conditions, have long life spans and produce a small number of offspring (Begon et al., 1996, 1998). A common group of K-strategists includes species of the genera *Abathomphalus*, *Archeoglobigerina*, *Contusotruncana*, *Globotruncana*, *Globotruncanita*, *Gublerina*, *Planoglobulina*, *Pseudoguembelina*, *Pseudotextularia*, *Racemiguembelina* and *Rugoglobigerina* (Premoli Silva and Sliter, 1999; Keller and Abramovich, 2009). These species are most abundant in stable environments with oligotrophic conditions, which foster optimum assemblages
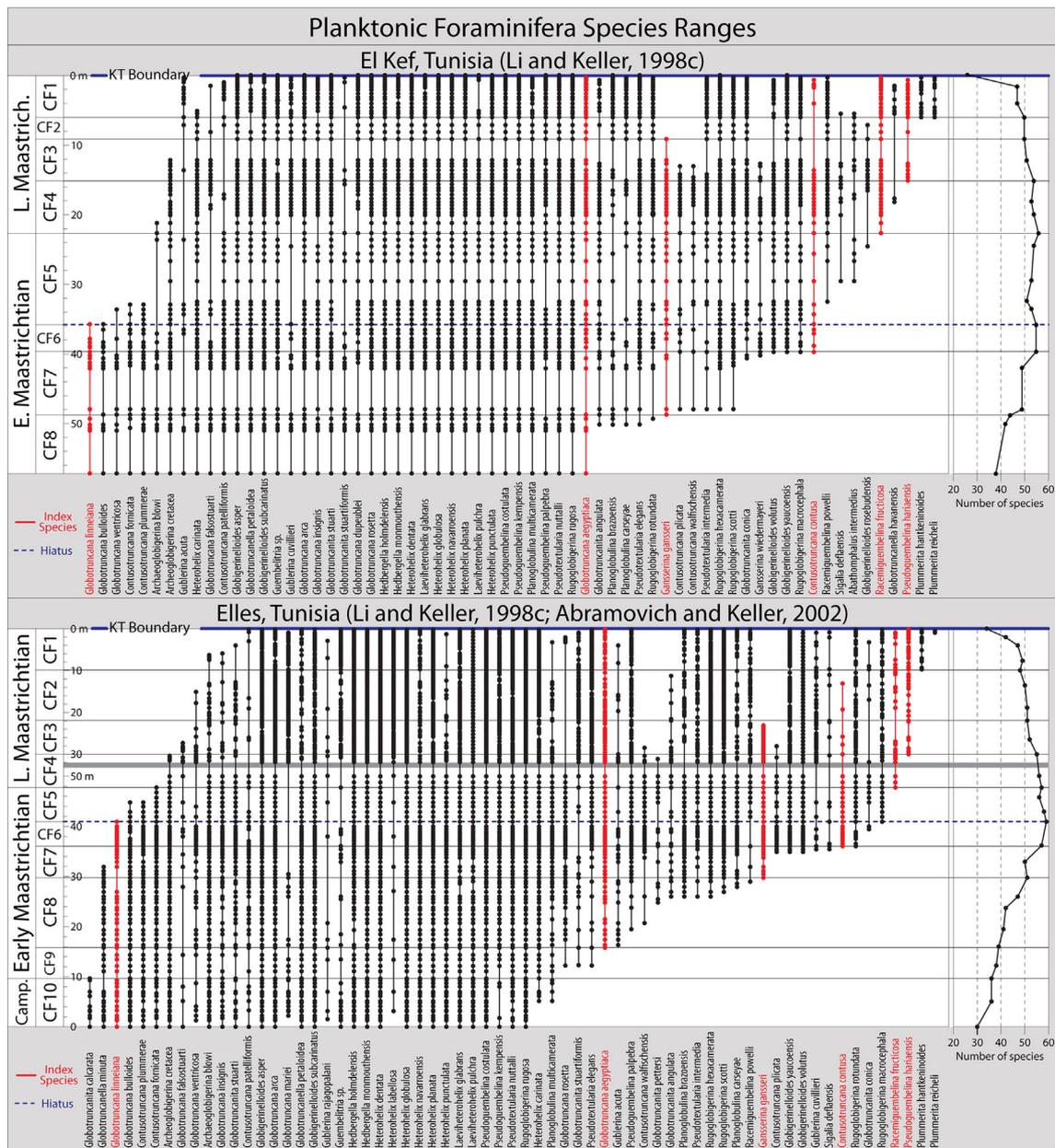
Fig. 8. Biostratigraphy of Maastrichtian planktic foraminifera at Elles and El Kef, Tunisia (Li and Keller, 1998c; Abramovich and Keller, 2002). Note rapid species originations in zones CF8–CF6 and a minor extinction event in zone CF5.

with high species diversity, a variety of test sizes, morphologies and ornamentation (e.g., Premoli Silva and Sliter, 1999; Pardo and Keller, 2008; Keller and Abramovich, 2009).

Generalist and disaster opportunist species are known as ecological R-strategists: low-diversity species assemblages with relatively small, simple tests, able to occupy a wide range of ecological niches, have shorter life spans and produce larger numbers of offspring, thus maximizing their chance for survival (Begon et al., 1996, 1998; Premoli Silva and Sliter, 1999; Keller and Abramovich, 2009). Generalists are represented by species of the genera *Globigerinelloides*, *Globotruncanella*, *Hedbergella* and *Heterohelix*. They tend to dominate high-stress environments affected by temperature, salinity, nutrients and oxygen variations in which large specialized species struggle to survive. *Heterohelix* species are common under mesotrophic conditions in low oxygen environments, usually thriving during times of an expanded oxygen minimum zone (OMZ) (Pardo and Keller, 2008), while *Globigerinelloides* species are most abundant in extreme eutrophic conditions (Ashckenazi-Polivoda et al., 2011). Disaster opportunists, such

as *Guembelitria* species, thrived under the most severe biotic stress conditions generally associated with mesotrophic to eutrophic conditions in shallow continental shelves, upwelling areas and volcanically influenced regions (e.g., Kroon and Nederbragt, 1990; Koutsoukos, 1994; Coccioni and Luciani, 2006; Pardo and Keller, 2008; Keller and Abramovich, 2009; Ashckenazi-Polivoda et al., 2014; Punekar et al., 2014a).

Planktic foraminifera also occupy a wide variety of ecological niches at various depths in the water column. Previous studies determined species depth ranking in the water column based on their oxygen and carbon isotopic signals and grouped them into surface, subsurface, thermocline and deep dwellers (Abramovich et al., 2003, 2011; Ashckenazi-Polivoda et al., 2014). Diversity and abundance changes for each depth group can be used to interpret changes in climate and water mass stratification as well as paleoecology.

At Site 217, generalist species dominate the 63–150 μm size fraction, particularly *Heterohelix* and *Globigerinelloides* species, which are most abundant from zone CF8 to CF5 and from zone CF4 to CF3, respectively
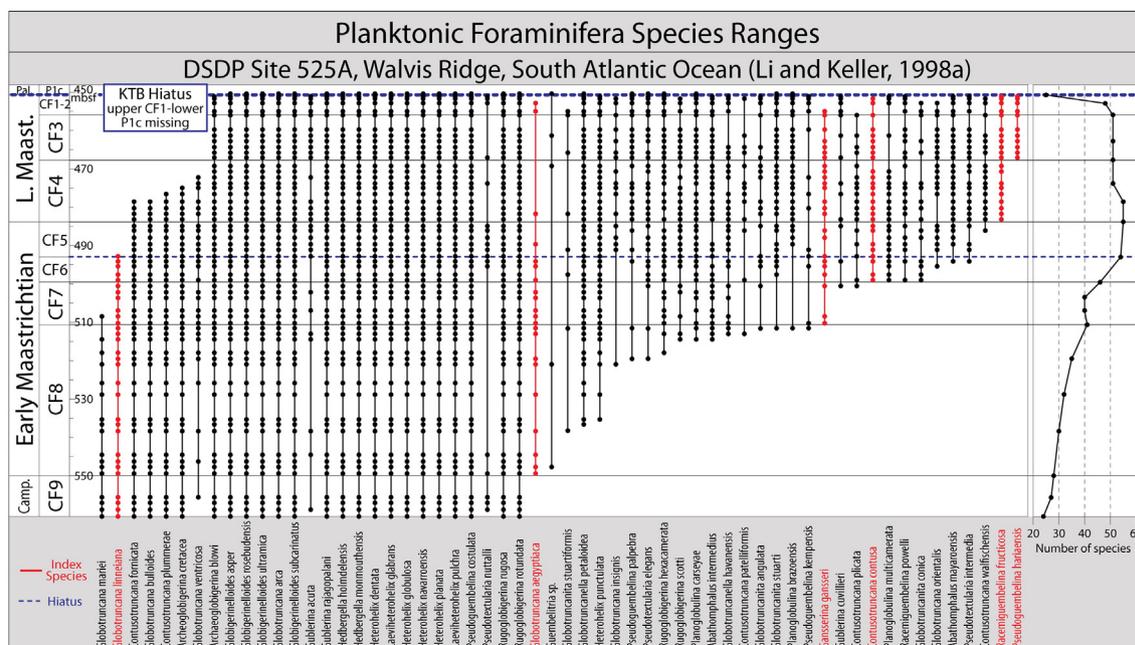
Fig. 9. Biostratigraphy of Maastrichtian planktic foraminifera at DSDP Site 525A, South Atlantic Ocean (Li and Keller, 1998a). Note rapid species originations in zones CF8–CF6 and a minor extinction event in zone CF4.

(Fig. 10), suggesting mesotrophic to eutrophic surface water conditions. A significant increase, from 4 % to 13 %, in *Globotruncanella* species is observed in zone CF3 in the predominantly smaller 63–150 μm size fraction, indicating dwarfing due to increased biotic stress. Specialist species are the second-most abundant group in the assemblage with dwarfed pseudoguembelinids dominating. Disaster opportunist *Guembelitria cretacea* is present throughout the section but rare (<1 %) except for the upper part of zone CF4 through CF3 and CF2 where relative abundances average 5 %; maximum peaks of 43 % are observed in zone CF2 in the dwarfed 38–63 μm size fraction (Fig. 10). This increased abundance indicates increasing environmental stress mainly in zones CF3–CF2 compared with the lower part of the section. Overall, dwarfed specialists (pseudoguembelinids), a marked faunal turnover at the CF4/CF3 transition, and presence of dwarfed *Guembelitria* with peak abundance in zone CF2 reveal increased biotic and environmental stress conditions from the early to the late Maastrichtian.

The >150 μm size fraction is dominated by specialist species with different degrees of environmental tolerance. Pseudoguembelinids, which are the only large surface dwellers with significant abundance, appear to be the most tolerant as evident by their maximum abundance (6.5 % to 32 %) during the increasingly high-stress environment of zones

CF3–CF2 (Fig. 11). In contrast, the subsurface and thermocline dwelling globotruncanids appear less tolerant of environmental fluctuations as indicated by their permanent decrease beginning in zone CF3. A similar lack of tolerance in CF3–CF2 environments is observed in the subsurface dwelling rugoglobigerinids. Reduced abundance of subsurface dwellers appears to be the result of reduced water mass stratification that led to decreased ecological niches and increased competition.

Small heterohelicids generally dominate among generalists, *H. globulosa, H. planata,* and *H.* (*Paraspiroplecta*) *navarroensis*, but *Gublerina rajagopalani,* a deep dweller, is the most abundant species in the larger >150 μm size fraction at Site 217 (Fig. 11). The high abundance of this large, robust and thick-walled species may be attributed primarily to selective preservation during carbonate dissolution. Noteworthy is the peak in the surface dweller *Guembelitria* in the 38–63 μm size fraction in zone CF2 (Fig. 10) coincident with dominance of large surface dwellers in the >150 μm size fraction (Fig. 11b), which suggests further reduction in habitats for deeper dwellers. Stable isotope ranking shows that *Guembelitria* thrived at the very sea-surface (Pardo and Keller, 2008; Abramovich et al., 2011; Ashckenazi-Polivoda et al., 2014) where CO_2 uptake from the air mitigates ocean acidification that affects other surface and

Table 1
Maastrichtian planktic foraminiferal species census data summary at DSDP Site 217, Cauvery Basin well Kali-H, India (Keller et al., 2016b), El Kef and Elles, Tunisia (Li and Keller, 1998c; Abramovich and Keller, 2002), and DSDP Site 525A (Li and Keller, 1998a). Note: N° of species per zone represent averages; some species may have been grouped or not recognized because of rarity, which may account for some variation in species richness. *Species that originate during the CF8a–CF5 diversification event (based on the complete records of Elles and Site 525A) but are not recorded, as the recovery of zone CF8a is incomplete.

| Location	Ninetyeast Ridge	SE India	Tunisia		South Atlantic
	DSDP Site 217	Well Kali-H	El Kef	Elles	DSDP Site 525A
Maximum diversity	60	61	56	59	55
CF8 - N° of species	54	48	42	47	36
CF7 - N° of species	58	54	49	51	45
CF6 - N° of species	59	59	55	58	52
CF5 - N° of species		60	53	58	53
CF4 - N° of species	60	61	55	56	52
CF3 - N° of species	56	56	54	52	51
CF2 - N° of species	54	Hiatus	51	51	49
CF1 - N° of species	Hiatus	Hiatus	49	47	45
N° of species originations Early Maastrichtian Zones CF8b–CF5	14 + 8* = 22	16 + 9* = 25	21	18	23
N° of species originations Early Maastrichtian Zones CF9–CF8a		Not recovered		7	6
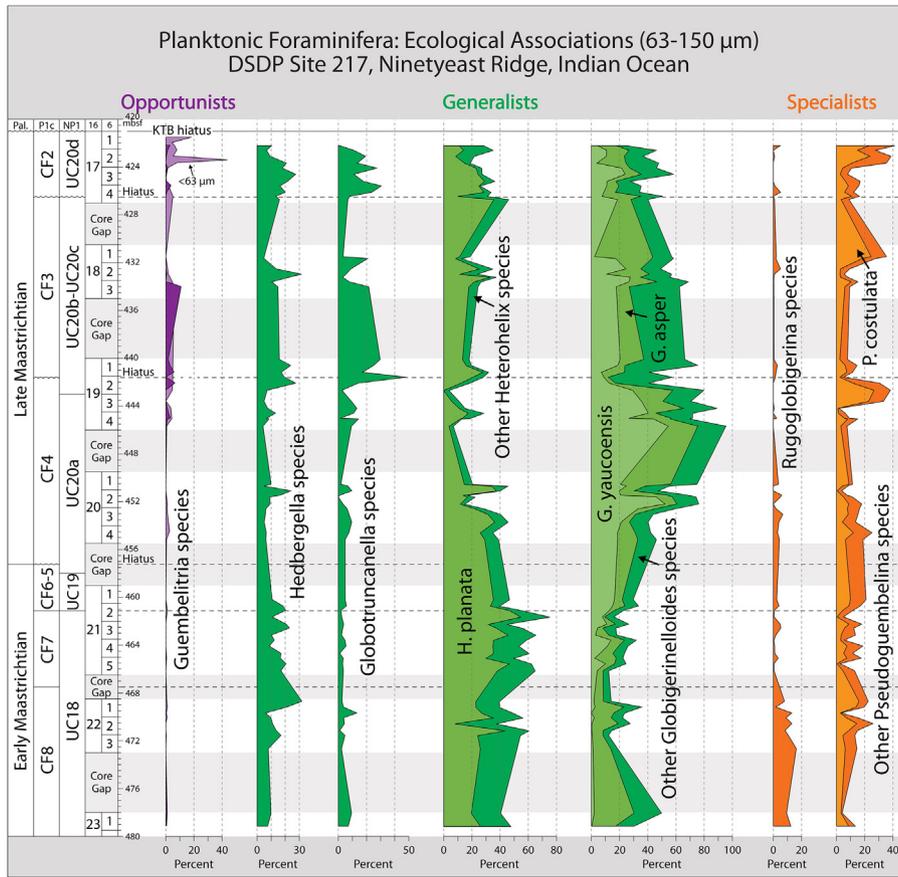
Fig. 10. Maastrichtian ecological associations of planktic foraminifera (63–150 μm size fraction) at Ninety East Ridge DSDP Site 217, Indian Ocean. Note increased abundance of the opportunist *Guembelitria* species (purple) and the generalist *Globotruncanella* species (green) in zone CF3 indicating increasingly high-stress environments and dwarfing. (For interpretation of the references to colour in this figure legend, the reader is referred to the web version of this article.)
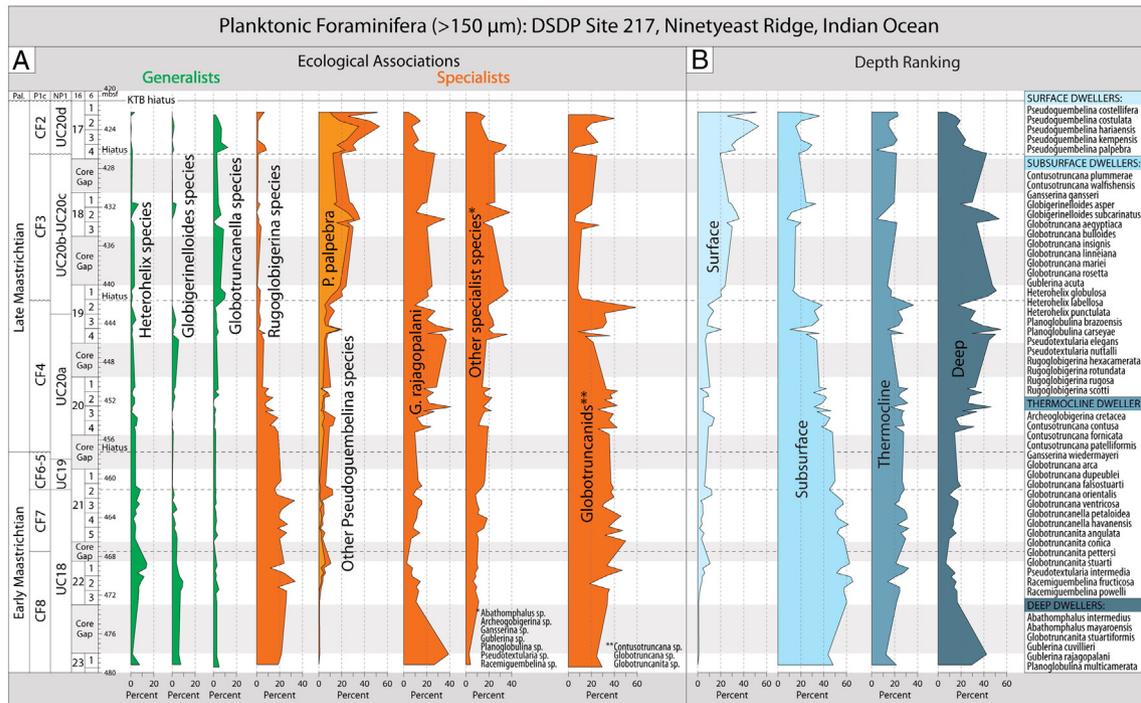

Fig. 11. A) Maastrichtian ecological associations and B) depth ranking of planktic foraminifera (>150 μm size fraction) at Ninety East Ridge DSDP Site 217, Indian Ocean. Note increased abundance of surface and deep dwelling species in zone CF3 indicating reduced water mass stratification. Depth ranking based on oxygen and carbon stable isotopes (Abramovich et al., 2003, 2011; Ashckenazi-Polivoda et al., 2014).

Please cite this article as: Mateo, P., et al., Early to Late Maastrichtian environmental changes in the Indian Ocean compared with Tethys and South Atlantic, Palaeogeogr. Palaeoclimatol. Palaeoecol. (2017), http://dx.doi.org/10.1016/j.palaeo.2017.01.027
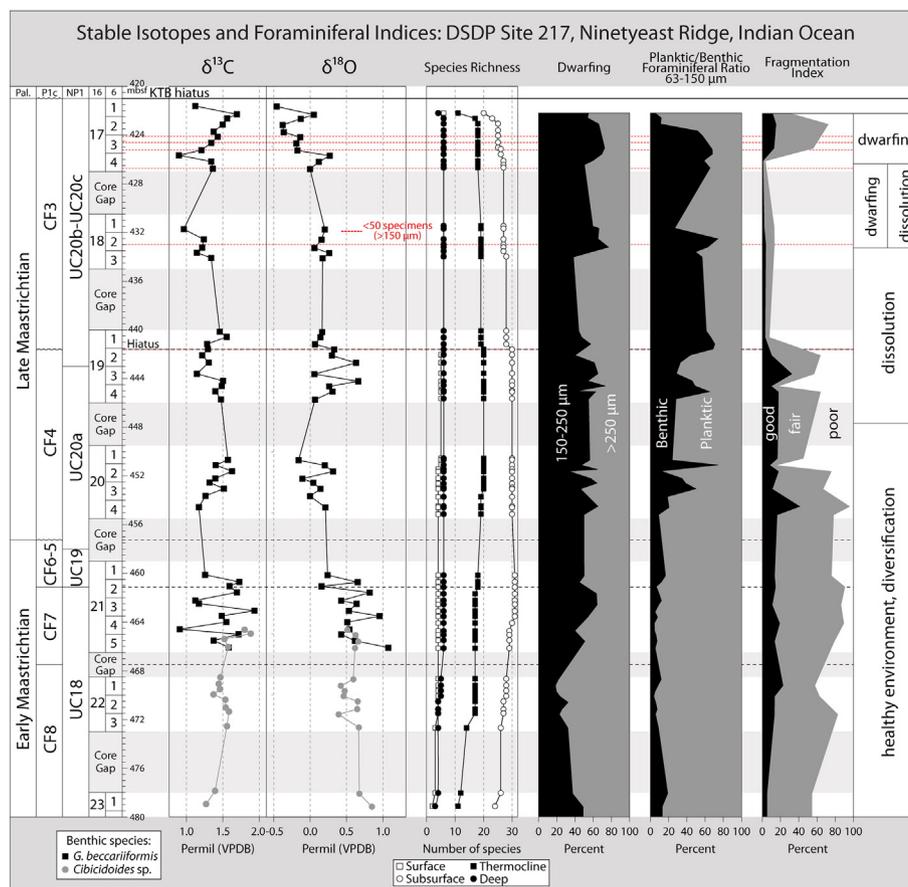
Fig. 12. Maastrichtian stable isotopic data of benthic foraminifera (*Gavelinella beccariiformis* and *Cibicidoides* species), species richness, dwarfing, planktic/benthic foraminiferal ratio (63–150 μm) and fragmentation index in Ninety East Ridge DSDP Site 217, Indian Ocean. Note increased dwarfing, increased abundance of benthic foraminifera and increased fragmentation in zone CF3 indicating increasingly high-stress environments and dissolution.

subsurface dwellers. All of these species population changes indicate increased high-stress environments beginning in CF4, increasing through CF3 and further increasing in CF2, as a result of reduced water mass stratification, reduced ecological niches and increased carbonate dissolution for planktic foraminifera.

6.2. Dwarfing

Species dwarfing refers to size reductions as a result of high-stress environments commonly associated with rapid climate change, perturbations in the water column and/or mesotrophic conditions (Abramovich and Keller, 2003; Keller and Abramovich, 2009). It is a survival response that enhances reproduction rates through early sexual maturation (i.e., organisms reach reproductive adulthood much below normal size; MacLeod et al., 2000; Keller and Abramovich, 2009).

At Site 217, there is a gradual trend throughout the section towards increased dwarfing suggesting a progressive increase in high-stress environmental conditions (Fig. 12). In zone CF8, the assemblage in the >150 μm size fraction is dominated by specimens >250 μm in size averaging 72 %. From zones CF7 to CF3, specimens in the 150–250 μm group are more abundant with an average of 52 %. In zone CF2, dwarfed specimens dominate averaging 60 % in the 150–250 μm group but several horizons have <50 specimens (e.g., 424.08 m, 424.59 m, 425.19 m, 426.70 m, 432.96 m). This indicates more severe environmental conditions associated with increased competition due to reduced water mass stratification and possibly carbonate dissolution. Similar results have been reported from wells in the Cauvery Basin, India, where planktic foraminifer diversity drops sharply and species tend to be dwarfed in the upper part of zone CF3 pointing to high biotic stress (Keller et al., 2016b).

6.3. Dissolution (Fragmentation index)

Preservation of planktic foraminiferal tests is mainly controlled by 1) seawater saturation with respect to $CaCO_3$ in the water column, and 2) the amount of organic matter buried in $CaCO_3$ rich sediments (e.g., Emerson and Bender, 1981). Dissolution is assessed based on 1) fragmentation index, 2) preferential preservation of robust planktic foraminiferal morphologies (species-selective dissolution), and 3) planktic/benthic (P/B) ratio of foraminifera (e.g., Parker and Berger, 1971; Thunell, 1976). The fragmentation index is calculated using the percentage of planktic foraminiferal fragments relative to the total number of whole tests and consists of three categories, "good", "fair" and "poor" based on the quality of preservation: good = nearly perfect tests, fair = imperfect tests, and poor = fragments (Punekar et al., 2016).

At Site 217, the "fair" group is the most abundant resulting in ~58 % from zone CF8 to the lower part of zone CF4 (Fig. 12). The "poor" group increases in the upper part of zone CF4 and dominates (91 %) in CF3. In contrast, zone CF2 is dominated by the "fair" group (~48 %), similar to lower CF4. Just below the hiatus in CF2 at the top of the section, the "poor" group dominates (70 %). The "good" group is a relatively minor component and maintains an average of only 13 %.

These results indicate that dissolution effects are most severe in zone CF3, as also evident by the dominance of robust, thick-walled and dissolution-resistant planktic species (e.g., *G. rajagopalani*, *P. palpebra* and *A. mayaroensis*, Fig. 3). Climate cooling in zone CF3 and the accompanying intensified bottom water circulation likely exacerbated effects of dissolution as suggested by the fragmentation of most foraminifera in this interval. Relative abundance of benthic compared to planktic foraminifera increase from 9 % in zones CF8–CF5 to 46 % in zone CF4 and dominate in zones CF3–CF2 with an average of 61 % (Fig. 12). These results reveal
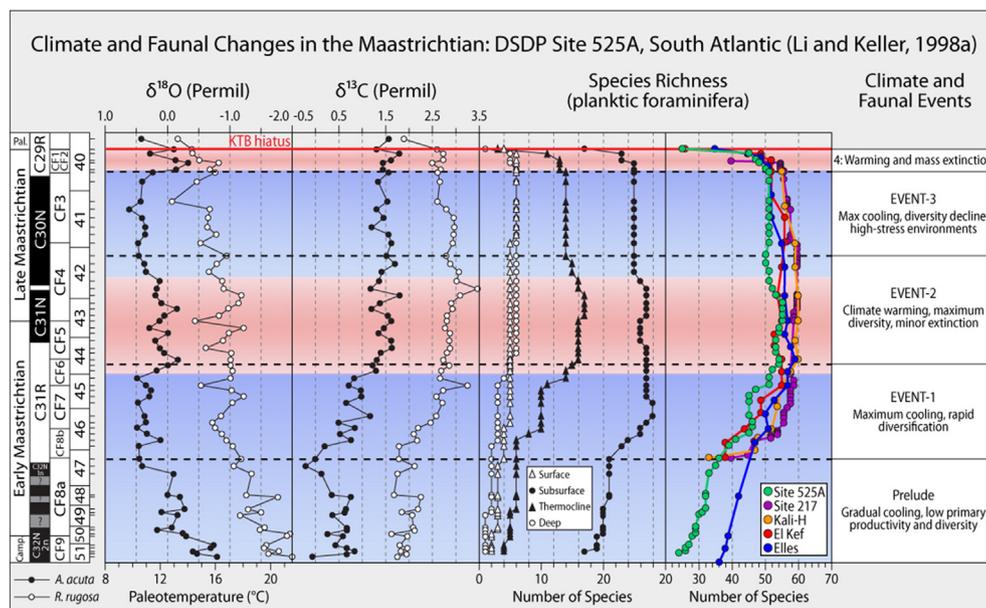
Fig. 13. Late Campanian-Maastrichtian climate, productivity and diversity changes based on planktic foraminifera at the South Atlantic DSDP Site 525A compared with species diversity from the Tethys (El Kef and Elles, Tunisia) and Indian Ocean (Site 217, Cauvery Basin). Four climatic and faunal events lead up to the K/T mass extinction revealing major upheavals in planktic foraminifera during the last 5 Myr of the Maastrichtian.

that at Site 217 increased dissolution actually started in zone CF4 and was persistent through CF2, as benthic foraminifera are less vulnerable to dissolution than planktic foraminifera. Planktic foraminifera dominate again (90 %) just below the KTB hiatus in zone CF2, coincident with increased abundance of surface dwellers, including peak abundance of the disaster opportunist *Guembelitria cretacea* (Figs. 10, 11). This suggests severe high-stress environmental conditions detrimental to all but sea-surface dwellers. Ocean acidification and reduced water mass stratification are likely contributors to the biotic stress that affected planktic foraminiferal assemblages during zones CF4–CF2.

7. Maastrichtian climate and faunal events

The Cretaceous greenhouse warming ended in the late Campanian with global cooling that reached minimum temperatures in the earliest Maastrichtian (base C31r) accompanied by low primary productivity and low diversity in planktic foraminifera (Fig. 13) (e.g., Li and Keller, 1998a; Huber et al., 2002; Friedrich et al., 2009). From the latest Campanian through the Maastrichtian, four major climate and faunal events are identified in the South Atlantic, Tethys and Indian Oceans: (1) minimum diversity in the late Campanian to earliest Maastrichtian followed by unprecedented diversification for the Cretaceous reaching maximum in the early Maastrichtian (Event-1, C31r), (2) a period of warming and stable high diversity (Event-2, upper C31r to lower C30n), (3) return to global cooling and high-stress environments (Event-3, C30n), and (4) rapid global warming and severe stress conditions in the late Maastrichtian preceding the K/T mass extinction (Event-4, C29r). Here we summarize these climate and faunal events based on stable isotopes and diversity records of South Atlantic Site 525A (Li and Keller, 1998a) compared with diversity curves from four localities in the Tethys and Indian oceans (Fig. 13).

7.1. Event-1: Early Maastrichtian cooling and diversification

The prelude to Event-1 is the late Campanian climate cooling (C32n, zones CF9–CF8) when bottom water temperatures dropped from 16 °C to 10 °C, surface water temperatures from 22 °C to 17 °C, and primary productivity and planktic foraminiferal diversity were relatively low (Fig. 13) (Li and Keller, 1998a). Event-1 spans most of the early

Maastrichtian (zones CF8b–CF6, C31r) with steady cold bottom water temperatures and gradual cooling of surface waters. $\delta^{13}C$ values rapidly increased by + 1 ‰ and + 1.4 ‰ in bottom and surface waters, respectively, indicating a major increase in primary productivity. Increasing primary productivity in the early Maastrichtian is also observed in northern middle to high latitudes as indicated by calcareous nannofossils and benthic foraminiferal assemblages (Friedrich et al., 2005). At Site 217, primary productivity was already high due to nutrient influx from Ninety East Ridge (Fig. 5). Planktic foraminifera responded with rapid evolutionary diversification among subsurface and thermocline dwellers (Fig. 13). Species originations vary from 45 % to 57 % (e.g., low of 35–42 to high of 55–61 species) among the five localities analyzed.

What could have caused the diversity decrease during the late Campanian cooling and the rapid diversification during the subsequent maximum cooling of the early Maastrichtian? The late Campanian cooling that ended the late Cretaceous greenhouse world is commonly attributed to a combination of declining atmospheric CO_2 related to decreasing oceanic crust production and the opening of ocean gateways that profoundly affected deep, intermediate and shallow waters circulation patterns (review in Linnert et al., 2014). Specialist planktic foraminifera were ill-suited to adapt to these environmental changes and many disappeared. By the earliest Maastrichtian maximum cooling, decreased diversity, reduced competition and high nutrient availability created favorable conditions for species originations (Li and Keller, 1998a, 1998c). High nutrient inputs were likely due to several factors including (1) increased temperature gradient between equator and poles favoring development of zonal winds and thus coastal upwelling of nutrient-rich waters (e.g., Vincent and Berger, 1985; Zachos et al., 1993), (2) increased erosion and nutrient influx from the continents during the sea-level lowstand ~70.6 Ma (Haq, 2014), and (3) nutrient inputs from Ninety East Ridge volcanic activity (e.g., Vermeij, 1995) active since ~82 Ma (Coffin et al., 2002; Pringle et al., 2008).

7.2. Event-2: Mid-Maastrichtian warming, maximum diversity, extinctions

Event-2, also known as mid-Maastrichtian event, begins near the end of the early Maastrichtian and persists through upper zones CF6 to middle CF4 (C31n) (Fig. 13). Bottom and surface waters warmed by

2–3 °C and terrestrial temperatures peaked at 22 °C (e.g., Li and Keller, 1998a; Zepeda, 1998; Nordt et al., 2003; Thibault and Gardin, 2007). High primary productivity and maximum diversity in planktic foraminifera persisted through this interval (Li and Keller, 1998a). The cause for this warming, attributed to abrupt reorganization of intermediate oceanic circulation, has long been an enigma (Frank and Arthur, 1999; Li and Keller, 1999), but recent studies suggest the cause could have been Ninety East Ridge volcanism (Keller et al., 2016a). An intense phase of volcanic activity is recorded at DSDP Site 216 beginning ~69.5 Ma and spanning zones CF5–CF3 coincident with persistent maximum diversity, high primary productivity, climate warming and increased water mass stratification favoring planktic foraminiferal evolution (Keller, 2005; Tantawy et al., 2009).

Deccan volcanism began near the end of Event-2 at the base of C30n (~67.1 Ma, Schöbel et al., 2014) further contributing to intense greenhouse warming and acid rains enhancing the delivery of nutrients to the oceans, thus resulting in mesotrophic conditions in surface waters favoring primary productivity. Faunal responses to these high-stress conditions include peak abundance of the disaster opportunist *Guembelitria cretacea*, and onset of the terminal decrease in large specialized globotruncanid species.

Enhanced weathering and probably waning volcanism eventually lowered volcanic CO_2 levels in the atmosphere resulting in climate cooling (e.g., Dessert et al., 2001), as observed in the upper part of zone CF4 (Fig. 13). Cooling would have further affected planktic foraminiferal assemblages by leading to reduced water mass stratification as temperature gradients between surface and deep waters decreased (e.g., Doney et al., 2012), thus resulting in reduced ecological niches and disappearance of some species (e.g., minor extinction event), marking the end of diversification.

7.3. Event-3: Late Maastrichtian cooling and diversity decline

Renewed global cooling during the late Maastrichtian upper zone CF4 to CF3 (C30n) marks Event-3 accompanied by sustained high primary productivity but increasingly high-stress marine environments for planktic foraminifera as a result of reduced ecological niches exacerbated by ocean acidification evident in increased carbonate dissolution effects (Figs. 12, 13). Faunal responses include species dwarfing, decreased populations of specialized species, temporary exclusions, dominance by generalist and/or disaster opportunist species and general diversity decrease, as observed in the Indian Ocean, Tethys and South Atlantic Oceans.

What caused the diversity decline during cooling in the late Maastrichtian instead of a diversity increase as observed during the early Maastrichtian cooling? Volcanism was active on Ninety East Ridge and in India (Deccan phase-1) but on relatively reduced levels during zone CF3 (C30n; Keller, 2005; Chenet et al., 2009) and insufficient to sustain global warming but sufficient to cause persistent ocean acidification, which stressed already reduced habitats. Large amounts of volcanogenic CO_2 adsorpt by the oceans changes seawater chemistry by lowering carbonate ion (CO_3^{2-}) concentration, surface ocean pH and saturation states of calcium carbonate minerals (Kump et al., 2009). The result is a carbonate crisis (i.e., decrease in $CaCO_3$ production) that significantly affects marine ecosystems, particularly marine calcifiers such as foraminifera (reviews in Doney et al., 2009; Hönisch et al., 2012). At Site 217, dissolution due to surface ocean acidification led to thinner planktic foraminiferal tests, thus more vulnerable to breakage (e.g., Moy et al., 2009), resulting in the high fragmentation index observed in zone CF3 (Fig. 12). Dissolution effects in other localities have not been routinely recorded and still have to be evaluated, although similar effects have been observed in zones CF4–CF3 in the Cauvery Basin (Keller et al., 2016b) and Site 525A (Punekar et al., unpublished data). Enhanced weathering and a major sea-level fall (~66.8 Ma) accompanied by widespread erosion also contributed to global cooling as well as increased nutrient input into the

oceans leading to mesotrophic conditions, detrimental to planktic foraminifera.

7.4. Event-4: Latest Maastrichtian rapid climate warming and mass extinction

Event-4 marks the last 250 kyr of the Maastrichtian (zones CF2–CF1, C29r), beginning with the largest Deccan eruptions (Phase-2) that caused rapid climate warming of 4 °C in bottom and surface waters and 8 °C on land, acid rain and ocean acidification leading to a major carbonate crisis thus contributing to the mass extinction (reviews in Punekar et al., 2014a; Keller et al., 2016a). This event is not present at Site 217 and rarely present in other Indian Ocean localities due to a major hiatus. The K/T boundary is also missing in the South Atlantic (DSDP Site 525A) and is fragmented in the Tethys (Egypt and Israel) although the best records are preserved in Tunisia (Fig. 2). This interval has been discussed in several recent publications in which Deccan volcanism is directly associated to the K/T mass extinction in India (Keller et al., 2011; Gertsch et al., 2011), U-Pb dating of lava flows narrow the main phase of eruptions to just 250 kyr below the KTB (Schoene et al., 2015), and global faunal and geochemical studies point to Deccan volcanism as a major trigger of the K/T mass extinction (e.g., Font et al., 2014, 2016; Punekar et al., 2014a, 2016), whereas others proposed a link between accelerated Deccan volcanism and the Chicxulub impact (Richards et al., 2015; Renne et al., 2015).

8. Conclusions

From the latest Campanian through the Maastrichtian, four major climate and faunal events are identified that ultimately ended with the K/T mass extinction.

- Event-1: Maximum cooling in the early Maastrichtian (zones CF8b-lower CF6; C31r) is associated with rapid planktic foraminiferal species originations reaching maximum Cretaceous diversity as a result of increased nutrient input due to enhanced upwelling, costal erosion and/or volcanic activity.
- Event-2: Warming during the early/late Maastrichtian transition (mid-Maastrichtian event; CF5 to lower CF4; upper C31r-C31n) is attributed to Ninety East Ridge volcanic activity that records an intense phase of eruptions at Site 216 in zones CF5–CF3. Warming led to increased water mass stratification that sustained maximum diversity.
- A minor extinction event ends Event 2 and marks the onset of increasingly more stressful marine conditions for planktic foraminifera particularly specialized species living in subsurface and thermocline depths.
- Event-3: Return to maximum cooling in zone CF3 (C30n) increased stress conditions for marine calcifiers leading to reduced specialized species populations, dwarfing, and dominance of smaller ecological generalists able to tolerate ongoing environmental changes. The global cooling and faunal turnover likely resulted from increased CO2 uptake by the oceans as a result of Ninety East Ridge and Deccan Trap volcanism, increased weathering after the greenhouse warming in the early-late Maastrichtian transition, ocean acidification and mesotrophic conditions.
- Event-4: Massive Deccan volcanic eruptions (phase-2) in zones CF2–CF1 spanning the last 250 kyr of the Maastrichtian (C29r) coincident with increasingly high-stress environments, decreasing abundance of large specialized species and dominance of the disaster opportunist *Guembelitria cretacea*. In the Indian Ocean, South Atlantic and eastern Tethys a major KTB hiatus is present.
- Positive and negative effects observed in planktic species diversification and population abundance variations through the Maastrichtian can be linked to volcanism. Positive effects correlate with increased nutrient input, increased water mass stratification and increased ecological niches during climate warming. Negative effects can be linked

to increased tempo and rate of volcanism resulting in ocean acidification, carbonate crisis and extinction.

Acknowledgments

References

Abramovich, S., Keller, G., 2002. High stress late Maastrichtian paleoenvironment: inference from planktonic foraminifera in Tunisia. Palaeogeogr. Palaeoclimatol. Palaeoecol. 178:145–164. http://dx.doi.org/10.1016/S0031-0182(01)00394-7.

Abramovich, S., Keller, G., 2003. Planktonic foraminiferal response to the latest Maastrichtian abrupt warm event: a case study from South Atlantic DSDP Site 525A. Mar. Micropaleontol. 48 (3–4):225–249. http://dx.doi.org/10.1016/S0377-8398(03)00021-5.

Abramovich, S., Almogi-Labin, A., Benjamini, C., 1998. Decline of the Maastrichtian pelagic ecosystem based on planktic foraminifera assemblage changes: implication for the terminal Cretaceous faunal crisis. Geology 26:63–66. http://dx.doi.org/10.1130/0091-7613(1998)026b0063:DOTMPEN2.3.CO;2.

Abramovich, S., Keller, G., Adatte, T., Stinnesbeck, W., Hottinger, L., Stüben, D., Berner, Z., Ramanivosoa, B., Randriamanantenasoa, A., 2002. Age and paleoenvironment of the Maastrichtian–Paleocene of the Mahajanga Basin, Madagascar: a multidisciplinary approach. Mar. Micropaleontol. 47:17–70. http://dx.doi.org/10.1016/S0377-8398(02)00094-4.

Abramovich, S., Keller, G., Stüben, D., Berner, Z., 2003. Characterization of late Campanian and Maastrichtian planktonic foraminiferal depth habitats and vital activities based on stable isotopes. Palaeogeogr. Palaeoclimatol. Palaeoecol. 202:1–29. http://dx.doi.org/10.1016/S0031-0182(03)00572-8.

Abramovich, S., Yovel-Corem, S., Almogi-Labin, A., Benjamini, C., 2010. Global climate change and planktic foraminiferal response in the Maastrichtian. Paleoceanography 25, PA2201. http://dx.doi.org/10.1029/2009PA001843.

Abramovich, S., Keller, G., Berner, Z., Cymbalista, M., Rak, C., 2011. Maastrichtian planktic foraminiferal biostratigraphy and paleoenvironment of Brazos River, Falls County, Texas. In: Keller, G., Adatte, T. (Eds.), The End-Cretaceous Mass Extinction and the Chicxulub Impact in Texas. Society for Sedimentary Geology Special Publication 100, pp. 123–156 (ISBN: 978-1-56576-308-1).

Alvarez, L.W., 1983. Experimental evidence that an asteroid impact led to the extinction of many species 65 million years ago. Proc. Natl. Acad. Sci. 80 (2), 627–642.

Alvarez, L.W., Alvarez, W., Asaro, F., Michel, H.V., 1980. Extraterrestrial cause for the Cretaceous-Tertiary extinction. Science 208:1095–1108. http://dx.doi.org/10.1126/science.208.4448.1095.

Arenillas, I., Arz, J.A., Grajales-Nishimura, J.M., Murillo-Muneton, G., Alvarez, W., Camargo-Zanguera, A., Molina, E., Rosales-Dominguez, C., 2006. Chicxulub impact event is Cretaceous/Paleogene boundary in age: new micropaleontological evidence. Earth Planet. Sci. Lett. 249:241–257. http://dx.doi.org/10.1016/j.epsl.2006.07.020.

Ashckenazi-Polivoda, S., Abramovich, S., Almogi-Labin, A., Schneider-Mor, A., Feinstein, S., Püttmann, W., Berner, Z., 2011. Paleoenvironments of the latest Cretaceous oil shale sequence, Southern Tethys, Israel, as an integral part of the prevailing upwelling system. Palaeogeogr. Palaeoclimatol. Palaeoecol. 305 (1):93–108. http://dx.doi.org/10.1016/j.palaeo.2011.02.018.

Ashckenazi-Polivoda, S., Rak, C., Almogi-Labin, A., Zsolt, B., Ovadia, O., Abramovich, S., 2014. Paleoecology of the K-Pg mass extinction survivor Guembelitria (Cushman): isotopic evidence from pristine foraminifera from Brazos River, Texas (Maastrichtian). Paleobiology 40 (1):24–33. http://dx.doi.org/10.1666/13317.

Barrera, E., 1994. Global environmental changes preceding the Cretaceous-Tertiary boundary: Early-late Maastrichtian transition. Geology 22 (10):877–880. http://dx.doi.org/10.1130/0091-7613(1994)022<0877:GECPTC>2.3.CO;2.

Barrera, E., Huber, B.T., 1990. Evolution of Antarctic waters during the Maastrichtian: Foraminifer oxygen and carbon isotope ratios, Leg 113. In: Barker, P.F., Kennett, J.P. (Eds.), Proceedings of the Ocean Drilling Program, Scientific Results, 113. College Station, Texas, Ocean Drilling Program, pp. 813–827.

Barrera, E., Savin, S.M., 1999. Evolution of late Campanian-Maastrichtian marine climates and oceans. In: Barrera, E., Johnson, C.C. (Eds.), Evolution of the Cretaceous Ocean-Climate System. Geological Society of America Special Papers 332, pp. 245–282.

Barrera, E., Huber, B.T., Savin, S.M., Webb, P.N., 1987. Antarctic marine temperatures: Late Campanian through early Paleocene. Paleoceanography 2 (1):21–47. http://dx.doi.org/10.1029/PA002i001p00021.

Begon, M., Mortimer, M., Thompson, D.J., 1996. Population Ecology: A Unified Study of Plants and Animals. Blackwell, Cambridge, UK (247 p).

Begon, M., Harper, J.L., Townsend, C.R., 1998. Ecology: Individuals, Populations and Communities. Blackwell Science, Boston (1068 p).

Bond, D.P.G., Wignall, P.B., 2014. Large igneous provinces and mass extinctions: an update. In: Keller, G., Kerr, A.C. (Eds.), Volcanism, Impacts, and Mass Extinctions: Causes and Effects. Geological Society of America Special Paper 505:pp. 29–55. http://dx.doi.org/10.1130/2014.2505(02).

Bralower, T.J., Paull, C.K., Leckie, R.M., 1998. The Cretaceous-Tertiary boundary cocktail: Chicxulub impact triggers margin collapse and extensive sediment gravity flows. Geology 26 (4):331–334. http://dx.doi.org/10.1130/0091-7613(1998)026<0331:TCTBCC>2.3.CO;2.

Burnett, J., 1998. Upper Cretaceous. In: Bown, P.R. (Ed.), Calcareous Nannofossil Biostratigraphy. Chapman & Hall, Cambridge, pp. 132–199.

Chenet, A.-L., Quidelleur, X., Fluteau, F., Courtillot, V., Bajpai, S., 2007. 40K/40Ar dating of the main Deccan large igneous province: further evidence of Cretaceous-Tertiary boundary age and short duration. Earth Planet. Sci. Lett. 263:1–15. http://dx.doi.org/10.1016/j.epsl.2007.07.011.

Chenet, A.-L., Fluteau, F., Courtillot, V., Gérard, M., Subbarao, K.V., 2008. Determination of rapid Deccan eruptions across the Cretaceous-Tertiary boundary using paleomagnetic secular variation: results from a 1200-m-thick section in the Mahabaleshwar escarpment. J. Geophys. Res. Solid Earth 113 (B4). http://dx.doi.org/10.1029/2006JB004635.

Chenet, A.-L., Courtillot, V., Fluteau, F., Gerard, M., Quidelleur, X., Khadri, S.F.R., Subbarao, K.V., Thordarson, T., 2009. Determination of rapid Deccan eruptions across the Cretaceous-Tertiary boundary using paleomagnetic secular variation: 2. Constraints from analysis of eight new sections and synthesis for a 3500-m-thick composite section. J. Geophys. Res. Solid Earth 114 (B6). http://dx.doi.org/10.1029/2008JB005644.

Coccioni, R., Luciani, V., 2006. Guembelitria irregularis bloom at the K-T boundary: morphological abnormalities induced in planktonic foraminifera by impact-related extreme environmental stress? In: Cockell, C., Gilmour, I., Koeberl, C. (Eds.), Biological Processes Associated with Impact Events. Springer-Verlag, Berlin, pp. 179–196.

Coffin, M.F., 1992. Emplacement and subsidence of Indian Ocean plateaus and submarine ridges. In: Duncan, R.A., et al. (Eds.), Synthesis of Results From Scientific Drilling in the Indian Ocean:pp. 115–125 http://dx.doi.org/10.1029/GM070p0115.

Coffin, M.F., Pringle, M.S., Duncan, R.A., Gladczenko, T.P., Storey, M., Müller, R.D., Gahagan, L.A., 2002. Kerguelen hotspot magma output since 130 Ma. J. Petrol. 43 (7): 1121–1137. http://dx.doi.org/10.1093/petrology/43.7.1121.

Courtillot, V., Fluteau, F., 2014. A review of the embedded time scales of flood basalt volcanism with special emphasis on dramatically short magmatic pulses. In: Keller, G., Kerr, A.C. (Eds.), Volcanism, Impacts, and Mass Extinctions: Causes and Effects. Geological Society of America Special Paper 505:pp. SPE505–SPE515. http://dx.doi.org/10.1130/2014.2505(15).

Courtillot, V., Renne, P.R., 2003. On the ages of flood basalt events. Compt. Rendus Geosci. 335 (1):113–140. http://dx.doi.org/10.1016/S1631-0713(03)00006-3.

Culver, S.J., 2003. Benthic foraminifera across the Cretaceous–Tertiary (K–T) boundary: a review. Mar. Micropaleontol. 47 (3):177–226. http://dx.doi.org/10.1016/S0377-8398(02)00117-2.

Darvishzad, B., Ghasemi-Nejad, E., Ghourchaei, S., Keller, G., 2007. Planktonic foraminiferal biostratigraphy and faunal turnover across the Cretaceous-Tertiary boundary in southwestern Iran. J. Sci., Islam. Repub. Iran 18 (2), 139–149.

Dessert, C., Dupré, B., François, L.M., Schott, J., Gaillardet, J., Chakrapani, G., Bajpai, S., 2001. Erosion of Deccan Traps determined by river geochemistry: impact on the global climate and the 87 Sr/86 Sr ratio of seawater. Earth Planet. Sci. Lett. 188 (3):459–474. http://dx.doi.org/10.1016/S0012-821X(01)00317-X.

D'Hondt, S., Arthur, M.A., 2002. Deep water in the Late Maastrichtian ocean. Paleoceanography 17 (1). http://dx.doi.org/10.1029/1999PA000486.

Doney, S.C., Fabry, V.J., Feely, R.A., Kleypas, J.A., 2009. Ocean acidification: the other CO2 problem. Annu. Rev. Mar. Sci. 1:169–192. http://dx.doi.org/10.1146/annurev.marine.010908.163834.

Doney, S.C., Ruckelshaus, M., Duffy, J.E., Barry, J.P., Chan, F., English, C.A., Galindo, H.M., Grebmeier, J.M., Hollowed, A.B., Knowlton, N., Polovina, J., Rabalais, N.N., Sydeman, W.J., Talley, L.D., 2012. Climate change impacts on marine ecosystems. Mar. Sci. 4: 11–37. http://dx.doi.org/10.1146/annurev-marine-041911-111611.

Douglas, R.G., Savin, S.M., 1975. Oxygen and carbon isotope analyses of Tertiary and Cretaceous microfossils from Shatsky Rise and other sites in the North Pacific Ocean. Initial Rep. Deep Sea Drill. Proj. 32:509–520. http://dx.doi.org/10.2973/dsdp.proc.32.115.1975.

Dubicka, Z., Peryt, D., 2012. The Lower/Upper Maastrichtian boundary interval in the Lublin Syncline (SE Poland, Boreal realm): new insight into foraminiferal stratigraphy. Newsl. Stratigr. 45 (2):139–150. http://dx.doi.org/10.1127/0078-0421/2012/0018.

Duncan, R.A., 1978. Geochronology of basalts from the Ninetyeast Ridge and continental dispersion in the eastern Indian Ocean. J. Volcanol. Geotherm. Res. 4:283–305. http://dx.doi.org/10.1016/0377-0273(78)90018-5.

Duncan, R.A., 1991. Age distribution of volcanism along aseismic ridges in the eastern Indian Ocean. Proc. Integr. Ocean Drill. Prog. 121:507–517. http://dx.doi.org/10.2973/odp.proc.sr.121.162.1991.

Emerson, S., Bender, M., 1981. Carbon fluxes at the sediment-water interface of the deepsea: calcium carbonate preservation. J. Mar. Res. 39, 139–162.

Eshet, Y., Almogi-Labin, A., 1996. Calcareous nannofossils as paleoproductivity indicators in Upper Cretaceous organic-rich sequences in Israel. Mar. Micropaleontol. 29 (1): 37–61. http://dx.doi.org/10.1016/0377-8398(96)00006-0.

Font, E., Fabre, S., Nédélec, A., Adatte, T., Keller, G., Veiga-Pires, C., Ponte, J., Mirão, J., Khozyem, H., Spangenberg, J.E., 2014. Atmospheric halogen and acid rains during the main phase of Deccan eruptions: magnetic and mineral evidence. In: Keller, G., Kerr, A.C. (Eds.), Volcanism, Impacts, and Mass Extinctions: Causes and Effects. Geological Society of America Special Paper 505:pp. 353–368. http://dx.doi.org/10.1130/2014.2505(18).

Font, E., Adatte, T., Sial, A.N., de Lacerda, L.D., Keller, G., Punekar, J., 2016. Mercury anomaly, Deccan volcanism, and the end-Cretaceous mass extinction. Geology 44 (2): 171–174. http://dx.doi.org/10.1130/G37451.1.

Frank, T.D., Arthur, M.A., 1999. Tectonic forcings of Maastrichtian ocean-climate evolution. Paleoceanography 14 (2):103–117. http://dx.doi.org/10.1029/1998PA900017.

Frank, T.D., Thomas, D.J., Leckie, R.M., Arthur, M.A., Brown, P.R., Jones, K., Lees, J.A., 2005. The Maastrichtian record from Shatsky Rise (northwest Pacific): a tropical perspective on global ecological and oceanographic changes. Paleoceanography 20, PA1008. http://dx.doi.org/10.1029/2004PA001052.

Friedrich, O., Herrle, J.O., Hemleben, C., 2005. Climatic changes in the Late Campanian-Early Maastrichtian: micropaleontological and stable isotopic evidence from an epicontinental sea. J. Foraminifer. Res. 35 (3):228–247. http://dx.doi.org/10.2113/35.3.228.

Friedrich, O., Schmiedl, G., Erlenkeuser, H., 2006. Stable isotope composition of Late Cretaceous benthic foraminifera from the southern South Atlantic: biological and environmental effects. Mar. Micropaleontol. 58:135–157. http://dx.doi.org/10.1016/j.marmicro.2005.10.005.

Friedrich, O., Herrle, J.O., Wilson, P.A., Cooper, M.J., Erbacher, J., Hemleben, C., 2009. Early Maastrichtian carbon cycle perturbation and cooling event: implications from the South Atlantic Ocean. Paleoceanography 24 (2), PA2211. http://dx.doi.org/10.1029/2008PA001654.

Gardin, S., Galbrun, B., Thibault, N., Coccioni, R., Premoli Silva, I., 2012. Biomagnetochronology for the upper Campanian–Maastrichtian from the Gubbio area, Italy: new results from the Contessa Highway and Bottaccione sections. Newsl. Stratigr. 45:75–100. http://dx.doi.org/10.1127/0078-0421/2012/0014.

Gertsch, B., Keller, G., Adatte, T., Garg, R., Prasad, V., Fleitmann, D., Berner, Z., 2011. Environmental effects of Deccan volcanism across the Cretaceous–Tertiary transition in Meghalaya, India. Earth Planet. Sci. Lett. 310:272–285. http://dx.doi.org/10.1016/j.epsl.2011.08.015.

Gradstein, F.M., Ogg, J.G., Schmitz, M., Ogg, G., 2012. The Geologic Time Scale 2012. Elsevier, Boston, USA:p. 1176 http://dx.doi.org/10.1016/B978-0-444-59425-9.00004-4.

Hallock, P., 1987. Fluctuations in the trophic resource continuum: a factor in global diversity cycles? Paleoceanography 2:457–471. http://dx.doi.org/10.1029/PA002i005p00457.

Haq, B.U., 2014. Cretaceous eustasy revisited. Glob. Planet. Chang. 113:44–58. http://dx.doi.org/10.1016/j.gloplacha.2013.12.007.

Haq, B.U., Hardenbol, J., Vail, P.R., 1987. Chronology of fluctuating sea levels since the Triassic. Science 235 (4793):1156–1167. http://dx.doi.org/10.1126/science.235.4793.1156.

Hart, M.B., 2007. Late Cretaceous climates and foraminiferid distributions. In: Williams, M., Haywood, A.M., Gregory, F.J., Schmidt, D.N. (Eds.), Deep-Time Perspectives on Climate Change: Marrying the Signal From Computer Models and Biological Proxies. Geological Society Special Publication 2, pp. 235–250.

Hildebrand, A.R., Penfield, G.T., Kring, D.A., Pilkington, M., Camargo, A., Jacobsen, S.B., Boynton, W.V., 1991. Chicxulub crater: a possible Cretaceous/Tertiary boundary impact crater on the Yucatan Peninsula, Mexico. Geology 19 (9):867–871. http://dx.doi.org/10.1130/0091-7613(1991)019<0867:CCAPCT>2.3.CO;2.

Hönisch, B., Ridgwell, A., Schmidt, D.N., Thomas, E., Gibbs, S.J., Sluijs, A., Zeebe, R., Kump, L., Martindale, R.C., Greene, S.E., Kiessling, G., Ries, J., Zachos, J.C., Royer, D.L., Barker, S., Marchitto Jr., T.M., Moyer, R., Pelejero, C., Ziveril, P., Foster, G.L., Williams, B., 2012. The geological record of ocean acidification. Science 335 (6072):1058–1063. http://dx.doi.org/10.1126/science.1208277.

Huber, B.T., Norris, R.D., MacLeod, K.G., 2002. Deep-sea paleotemperature record of extreme warmth during the Cretaceous. Geology 30 (2):123–126. http://dx.doi.org/10.1130/0091-7613(2002)030<0123:DSPROE>2.0.CO;2.

Huber, B.T., MacLeod, K.G., Tur, N.A., 2008. Chronostratigraphic framework for upper Campanian-Maastrichtian sediments on the Blake Nose (subtropical North Atlantic). J. Foraminifer. Res. 38:162–182. http://dx.doi.org/10.2113/gsjfr.38.2.162.

Husson, D., Galbrun, B., Laskar, J., Hinnov, L.A., Thibault, N., Gardin, S., Locklair, R.E., 2011. Astronomical calibration of the Maastrichtian (Late Cretaceous). Earth Planet. Sci. Lett. 305:328–340. http://dx.doi.org/10.1016/j.epsl.2011.03.008.

Isaza-Londoño, C., MacLeod, K.G., Huber, B.T., 2006. Maastrichtian North Atlantic warming, increasing stratification, and foraminiferal paleobiology at three timescales. Paleoceanography 21, PA1012. http://dx.doi.org/10.1029/2004PA001130.

Izett, G.A., 1990. The Cretaceous/Tertiary boundary interval, Raton Basin, Colorado and New Mexico, and its content of shock-metamorphosed minerals; evidence relevant to the K/T boundary impact-extinction theory. Geol. Soc. Am. Spec. Pap. 249:1–100. http://dx.doi.org/10.1130/SPE249-p1.

Keller, G., 2005. Biotic effects of late Maastrichtian mantle plume volcanism: implications for impacts and mass extinctions. Lithos 79 (3–4):317–341. http://dx.doi.org/10.1016/j.lithos.2004.09.005.

Keller, G., Kerr, A.C., 2014. Deccan volcanism, the Chicxulub impact, and the end-Cretaceous mass extinction: coincidence? Cause and effect? In: Keller, G. (Ed.), Volcanism, Impacts, and Mass Extinctions: Causes and Effects. Geological Society of America Special Paper 505:pp. 57–89. http://dx.doi.org/10.1130/2014.2505(03)

Keller, G., Abramovich, S., 2009. Lilliput effect in Late Maastrichtian planktic foraminifera: response to environmental stress. Palaeogeogr. Palaeoclimatol. Palaeoecol. 284: 47–62. http://dx.doi.org/10.1016/j.palaeo.2009.08.029.

Keller, G., Adatte, T., Burns, S.J., Tantawy, A.A., 2002. High-stress paleoenvironment during the late Maastrichtian to early Paleocene in central Egypt. Palaeogeogr. Palaeoclimatol. Palaeoecol. 187:35–60. http://dx.doi.org/10.1016/S0031-0182(02)00504-7.

Keller, G., Bhowmick, P.K., Upadhyay, H., Dave, A., Reddy, A.N., Jaiprakash, B.C., Adatte, T., 2011. Deccan volcanism linked to the Cretaceous-Tertiary boundary (KTB) mass extinction: new evidence from ONGC wells in the Krishna-Godavari Basin, India. J. Geol. Soc. India 78:399–428. http://dx.doi.org/10.1007/s12594-011-0107-3.

Keller, G., Khozyem, H.M., Adatte, T., Malarkodi, N., Spangenberg, J.E., Stinnesbeck, W., 2013. Chicxulub impact spherules in the North Atlantic and Caribbean: age constraints and Cretaceous-Tertiary boundary hiatus. Geol. Mag. 150 (05):885–907. http://dx.doi.org/10.1017/S0016756812001069.

Keller, G., Punekar, J., Mateo, P., 2016a. Upheavals during the late Maastrichtian: volcanism, climate and faunal events preceding the end-Cretaceous mass extinction. Palaeogeogr. Palaeoclimatol. Palaeoecol. 441:137–151. http://dx.doi.org/10.1016/j.palaeo.2015.06.034.

Keller, G., Jaiprakash, B.C., Reddy, A.N., 2016b. Maastrichtian to Eocene subsurface stratigraphy of the Cauvery basin and correlation with Madagascar. J. Geol. Soc. India 87 (1): 5–34. http://dx.doi.org/10.1007/s12594-016-0370-4.

Koutsoukos, E.A.M., 1994. Early stratigraphic record and phylogeny of the planktonic genus Guembelitria Cushman, 1933. J. Foraminifer. Res. 24:288–295. http://dx.doi.org/10.2113/gsjfr.24.4.288.

Kring, D.A., 2007. The Chicxulub impact event and its environmental consequences at the Cretaceous–Tertiary boundary. Palaeogeogr. Palaeoclimatol. Palaeoecol. 255 (1): 4–21. http://dx.doi.org/10.1016/j.palaeo.2007.02.037.

Krishna, K.S., Abraham, H., Sager, W.W., Pringle, M.S., Frey, F., Gopala Rao, D., Levchenko, O.V., 2012. Tectonics of the Ninetyeast Ridge derived from spreading records in adjacent oceanic basins and age constraints of the ridge. J. Geophys. Res. 117, B04101. http://dx.doi.org/10.1029/2011JB008805.

Kroon, D., Nederbragt, A.J., 1990. Ecology and paleoecology of triserial planktic foraminifera. Mar. Micropaleontol. 16:25–38. http://dx.doi.org/10.1016/0377-8398(90)90027-J.

Kump, L., Bralower, T., Ridgwell, A., 2009. Ocean acidification in deep time. Oceanography 22 (4), 94–107.

Leckie, R.M., 1987. Paleoecology of mid-Cretaceous planktonic foraminifera: a comparison of open ocean and epicontinental sea assemblages. Micropaleontology 33 (2): 164–176. http://dx.doi.org/10.2307/1485491.

Li, L., Keller, G., 1998a. Maastrichtian climate, productivity and faunal turnovers in planktic foraminifera of South Atlantic DSDP Sites 525A and 21. Mar. Micropaleontol. 33 (1–2):55–86. http://dx.doi.org/10.1016/S0377-8398(97)00027-3.

Li, L., Keller, G., 1998b. Abrupt deep-sea warming at the end of the Cretaceous. Geology 26:995–998. http://dx.doi.org/10.1130/0091-7613(1998)026<0995:ADSWAT>2.3.CO;2.

Li, L., Keller, G., 1998c. Diversification and extinction in Campanian-Maastrichtian planktic foraminifera of northwestern Tunisia. Eclogae Geol. Helv. 91 (1), 75–102.

Li, L., Keller, G., 1999. Variability in Late Cretaceous climate and deep waters: evidence from stable isotopes. Mar. Geol. 161:171–190. http://dx.doi.org/10.1016/S0025-3227(99)00078-X.

Li, L., Keller, G., Adatte, T., Stinnesbeck, W., 2000. Late Cretaceous sea-level changes in Tunisia: a multi-disciplinary approach. J. Geol. Soc. Lond. 157:447–458. http://dx.doi.org/10.1144/jgs.157.2.447.

Linnert, C., Robinson, S.A., Lees, J.A., Bown, P.R., Pérez-Rodríguez, I., Petrizzo, M.R., Falzoni, F., Littler, K., Arz, J.A., Russell, E.E., 2014. Evidence for global cooling in the Late Cretaceous. Nat. Commun. 5:4194. http://dx.doi.org/10.1038/ncomms5194.

Luyendyk, B.P., 1977. Deep sea drilling on the Ninetyeast Ridge: synthesis and a tectonic model. In: Heirtzler, J.R., Bolli, H.M., Davies, T.A., Saunders, J.B., Sclater, J.C. (Eds.), Indian Ocean Geology and Biostratigraphy. American Geophysical Union, Washington, D.C. http://dx.doi.org/10.1029/SP009p0165.

MacLeod, K.G., 1994. Bioturbation, inoceramid extinction, and mid-Maastrichtian ecological change. Geology 22:139–142. http://dx.doi.org/10.1130/0091-7613(1994)022<0139:BIEAMM>2.3.CO;2.

MacLeod, N., Keller, G., 1991. Hiatus distributions and mass extinctions at the Cretaceous/Tertiary boundary. Geology 19:497–501. http://dx.doi.org/10.1130/0091-7613(1991)019b0497:HDAMEAN2.3.CO;2.

MacLeod, N., Ortiz, N., Fefferman, N., Clyde, W., Schulter, C., MacLean, J., 2000. Phenotypic response of foraminifera to episodes of global environmental change. In: Culver, S.J., Rawson, P. (Eds.), Biotic Response to Global Environmental Change: The Last 145 Million Years. Cambridge University Press, Cambridge, UK, pp. 51–78.

MacLeod, K.G., Huber, B.T., Pletsch, T., Röhl, U., Kucera, M., 2001. Maastrichtian foraminiferal and paleoceanographic changes on Milankovitch timescales. Paleoceanography 16 (2):133–154. http://dx.doi.org/10.1029/2000PA000514.

MacLeod, K.G., Huber, B.T., Isaza-Londoño, C., 2005. North Atlantic warming during "global" cooling at the end of the Cretaceous. Geology 33:437–440. http://dx.doi.org/10.1130/G21466.1.

MacLeod, K.G., Whitney, D.L., Huber, B.T., Koeberl, C., 2007. Impact and extinction in remarkably complete Cretaceous-Tertiary boundary sections from Demerara Rise, tropical western North Atlantic. Geol. Soc. Am. Bull. 119 (1–2):101–115. http://dx.doi.org/10.1130/B25955.1.

Malmgren, B.A., 1987. Differential dissolution of Upper Cretaceous planktonic foraminifera from a temperate region of the South Atlantic Ocean. Mar. Micropaleontol. 11 (4):251–271. http://dx.doi.org/10.1016/0377-8398(87)90001-6.

Mateo, P., Keller, G., Adatte, T., Spangenberg, J.E., 2016. Mass wasting and hiatuses during the Cretaceous-Tertiary transition in the North Atlantic: relationship to the Chicxulub impact? Palaeogeogr. Palaeoclimatol. Palaeoecol. 441:96–115. http://dx.doi.org/10.1016/j.palaeo.2015.01.019.

Meilijson, A., Ashckenazi-Polivoda, S., Ron-Yankovich, L., Illner, P., Alsenz, H., Speijer, R.P., Almogi-Labin, A., Feinstein, S., Berner, Z., Püttmann, W., Abramovich, S., 2014. Chronostratigraphy of the Upper Cretaceous high productivity sequence of the southern Tethys, Israel. Cretac. Res. 50:187–213. http://dx.doi.org/10.1016/j.cretres.2014.04.006.

Moore, D.G., Curray, J.R., Raitt, R.W., Emmel, F.J., 1974. Stratigraphic-seismic sections correlations and implications to Bengal fan history. In: von der Borch, C.C., Slater,

J.G., et al. (Eds.), Initial Reports of the Deep Sea Drilling Project, 22. U.S. Government Printing Office, Washington:pp. 403–412 http://dx.doi.org/10.2973/dsdp.proc.22.116.1974.

Moy, A.D., Howard, W.R., Bray, S.G., Trull, T.W., 2009. Reduced calcification in modern Southern Ocean planktonic foraminifera. Nat. Geosci. 2 (4):276–280. http://dx.doi.org/10.1038/ngeo460.

Nederbragt, A.J., 1991. Late Cretaceous biostratigraphy and development of Heterohelicidae (planktic foraminifera). Micropaleontology 37 (4):329–372. http://dx.doi.org/10.2307/1485910.

Nordt, L., Atchley, S., Dworkin, S., 2003. Terrestrial evidence for two greenhouse events in the latest Cretaceous. GSA Today 13 (12):4–9. http://dx.doi.org/10.1130/1052-5173(2003)013<4:TEFTGE>2.0.CO;2.

Norris, R.D., Huber, B.T., Self-Trail, J., 1999. Synchroneity of the KT oceanic mass extinction and meteorite impact: Blake Nose, western North Atlantic. Geology 27 (5):419–422. http://dx.doi.org/10.1130/0091-7613(1999)027<0419:SOTKTO>2.3.CO;2.

Olsson, R.K., Miller, K.G., Browning, J.V., Habib, D., Sugarmann, P.J., 1997. Ejecta layer at the Cretaceous-Tertiary boundary, Bass River, New Jersey (Ocean Drilling Program Leg 174AX). Geology 25 (8):759–762. http://dx.doi.org/10.1130/0091-7613(1997)025<0759:ELATCT>2.3.CO;2.

Olsson, R.K., Hemleben, C., Berggren, W.A., Huber, B.T., 1999. Atlas of Paleocene Planktonic Foraminifera. Smithsonian Contributions to Paleobiology, 85. Smithsonian Institution Press, Washington, DC, p. 252.

Olsson, R.K., Wright, J.D., Miller, K.G., 2001. Paleobiogeography of *Pseudotextularia elegans* during the latest Maastrichtian global warming event. J. Foraminifer. Res. 31: 275–282. http://dx.doi.org/10.2113/31.3.275.

Pardo, A., Keller, G., 2008. Biotic effects of environmental catastrophes at the end of the Cretaceous: Guembelitria and Heterohelix blooms. Cretac. Res. 29 (5–6): 1058–1073. http://dx.doi.org/10.1016/j.cretres.2008.05.031.

Parker, F.L., Berger, W.H., 1971. Faunal and solution patterns of planktonic foraminifera in surface sediments of the South Pacific. Deep Sea Res. Oceanogr. Abstr. 18 (1):73–107. http://dx.doi.org/10.1016/0011-7471(71)90017-9.

Premoli Silva, I., Sliter, W.V., 1999. Cretaceous paleoceanography: evidence from planktonic foraminiferal evolution. Special Papers-Geological Society of America, pp. 301–328.

Pringle, M.S., Frey, F.A., Mervine, E.M., 2008. A simple linear age progression for the Ninetyeast Ridge, Indian Ocean: new constraints on Indian plate tectonics and hotspot dynamics. Eos Transactions AGU Fall Meeting Supplementary Abstract. 89, pp. T54B–T503.

Punekar, J., Mateo, P., Keller, G., 2014a. Effects of Deccan volcanism on paleoenvironment and planktic foraminifera: a global survey. In: Keller, G., Kerr, A.C. (Eds.), Volcanism, Impacts, and Mass Extinctions: Causes and Effects. Geological Society of America Special Paper 505:pp. 91–116. http://dx.doi.org/10.1130/2014.2505(04).

Punekar, J., Keller, G., Khozyem, H.M., Hamming, C., Adatte, T., Tantawy, A.A., Spangenberg, J., 2014b. Late Maastrichtian-early Danian high-stress environments and delayed recovery linked to Deccan volcanism. Cretac. Res. 49:63–82. http://dx.doi.org/10.1016/j.cretres.2014.01.002.

Punekar, J., Keller, G., Khozyem, H.M., Adatte, T., Font, E., Spangenberg, J., 2016. A multi-proxy approach to decode the end-Cretaceous mass extinction. Palaeogeogr. Palaeoclimatol. Palaeoecol. 441:116–136. http://dx.doi.org/10.1016/j.palaeo.2015.08.025.

Renne, P.R., Sprain, C.J., Richards, M.A., Self, S., Vanderkluysen, L., Pande, K., 2015. State shift in Deccan volcanism at the Cretaceous-Paleogene boundary, possibly induced by impact. Science 350 (6256):76–78. http://dx.doi.org/10.1126/science.aac7549.

Richards, M.A., Alvarez, W., Self, S., Karlstrom, L., Renne, P.R., Manga, M., Sprain, C.J., Smit, J., Vanderkluysen, L., Gibson, S.A., 2015. Triggering of the largest Deccan eruptions by the Chicxulub impact. Geol. Soc. Am. Bull. 127 (11–12):1507–1520. http://dx.doi.org/10.1130/B31167.1.

Robaszynski, F., Caron, M., Gonzalez Donoso, J.M., Wonders, A.A.H., 1983-1984. Atlas of Late Cretaceous globotruncanids. Micropaleontology 26 (3–4), 145–305.

Rocchia, R., Robin, E., Froget, L., Gayraud, J., 1996. Stratigraphic distribution of extraterrestrial markers at the Cretaceous–Tertiary boundary in the Gulf of Mexico area: implications for the temporal complexity of the event. In: Ryder, G., Fastovsky, D., Gartner, S. (Eds.), The Cretaceous-Tertiary Event and Other Catastrophes in Earth History. Geological Society of America, Special Papers 307, pp. 279–286.

Schöbel, S., deWall, H., Ganerød, M., Pandit, M.K., Rolf, C., 2014. Magnetostratigraphy and 40Ar–39Ar geochronology of the Malwa Plateau region (Northern Deccan Traps), central western India: significance and correlation with the main Deccan Large Igneous Province sequences. J. Asian Earth Sci. 89:28–45. http://dx.doi.org/10.1016/j.jseaes.2014.03.022.

Schoene, B., Samperton, K.M., Eddy, M.P., Keller, G., Adatte, T., Bowring, S.A., Khadri, S.F.R., Gertsch, B., 2015. U–Pb geochronology of the Deccan Traps and relation to the end-Cretaceous mass extinction. Science 347:182–184. http://dx.doi.org/10.1126/science.aaa0118.

Schrag, D.P., DePaolo, D.J., Richter, F.M., 1995. Reconstructing past sea surface temperatures from oxygen isotope measurements of bulk carbonate. Geochim. Cosmochim. Acta 59:2265–2278. http://dx.doi.org/10.1016/0016-7037(95)00105-9.

Schulte, P., Alegret, L., Arenillas, I., Arz, J.A., Barton, P.J., Bown, P.R., Bralower, T.J., Christeson, G.L., Claeys, P., Cockell, C.S., Collins, G.S., Deutsch, A., Goldin, T.J., Goto, K., Grajales-Nishimura, J.M., Grieve, R.A.F., Gulick, S.P.S., Johnson, K.R., Kiessling, W., Koeberl, C., Kring, D.A., MacLeod, K.G., Matsui, T., Melosh, J., Montanari, A., Morgan, J.V., Neal, C.R., Nichols, D.J., Norris, R.D., Pierazzo, E., Ravizza, G., Rebolledo-Vieyra, M., Reimold, W.U., Robin, E., Salge, T., Speijer, R.P., Sweet, A.R., Urrutia-Fucugauchi, J., Vajda, V., Whalen, M.T., Willumsen, P.S., 2010. The Chicxulub asteroid impact and mass extinction at the Cretaceous-Paleogene boundary. Science 327:1214–1218. http://dx.doi.org/10.1126/science.1177265.

Schultz, P.H., D'Hondt, S., 1996. Cretaceous-Tertiary (Chicxulub) impact angle and its consequences. Geology 24 (11):963–967. http://dx.doi.org/10.1130/0091-7613(1996)024<0963:CTCIAA>2.3.CO;2.

Sclater, J.G., Fisher, R.L., 1974. Evolution of the East Central Indian Ocean, with emphasis on the tectonic setting of the Ninetyeast Ridge. Geol. Soc. Am. Bull. 85 (5):683–702. http://dx.doi.org/10.1130/0016-7606(1974)85<683:EOTECI>2.0.CO;2.

Scotese, C.R., 2013. Map Folio 16, KT boundary (65.5 Ma, latest Maastrichtian). PALEOMAP PaleoAtlas for ArcGIS, volume 2, Cretaceous, PALEOMAP Project, Evanston, IL.

Self, S., Jay, A.E., Widdowson, M., Keszthelyi, L.P., 2008. Correlation of the Deccan and Rajahmundry Trap lavas: are these the longest and largest lava flows on earth? J. Volcanol. Geotherm. Res. 172:3–19. http://dx.doi.org/10.1016/j.jvolgeores.2006.11.012.

Shackleton, N.J., 1987. Oxygen isotopes, ice volume and sea level. Quat. Sci. Rev. 6 (3–4): 183–190. http://dx.doi.org/10.1016/0277-3791(87)90003-5.

Smit, J., 1999. The global stratigraphy of the Cretaceous/Tertiary boundary impact ejecta. Annu. Rev. Earth Planet. Sci. 27:75–91. http://dx.doi.org/10.1146/annurev.earth.27.1.75.

Smit, J., Montanari, A., Swinburne, N.H.M., Alvarez, W., Hildebrand, A.R., Margolis, S.V., Claeys, P., Lowrie, W., Asaro, F., 1992. Tektite-bearing, deep-water clastic unit at the Cretaceous-Tertiary boundary in northeastern Mexico. Geology 20, 99–103.

Smit, J., Roep, T.B., Alvarez, W., Montanari, A., Claeys, P., Grajalesnishimura, J.M., Bermudez, J., 1996. Coarse-grained clastic sandstone complex at the K/T boundary around the Gulf of Mexico: deposition by tsunami waves induced by the Chicxulub impact? In: Ryder, G., Fastovsky, D., Gartner, S. (Eds.), The Cretaceous-Tertiary Event and other Catastrophes in Earth History. Geological Society of America Special Paper 307:pp. 151–182. http://dx.doi.org/10.1130/0-8137-2307-8.151

Tantawy, A.A., Keller, G., Pardo, A., 2009. Late Maastrichtian volcanism in the Indian Ocean: effects on calcareous nannofossils and planktic foraminifera. Palaeogeogr. Palaeoclimatol. Palaeoecol. 284:63–87. http://dx.doi.org/10.1016/j.palaeo.2009.08.025.

Thibault, N., 2016. Calcareous nannofossil biostratigraphy and turnover dynamics in the late Campanian–Maastrichtian of the tropical South Atlantic. Rev. Micropaleontol. 59 (1):57–69. http://dx.doi.org/10.1016/j.revmic.2016.01.001.

Thibault, N., Gardin, S., 2007. The late Maastrichtian nannofossil record of climate change in the South Atlantic DSDP Hole 525A. Mar. Micropaleontol. 65:163–184. http://dx.doi.org/10.1016/j.marmicro.2007.07.004.

Thibault, N., Gardin, S., 2010. The calcareous nannofossil response to the end-Cretaceous warm event in the Tropical Pacific. Palaeogeogr. Palaeoclimatol. Palaeoecol. 291: 239–252. http://dx.doi.org/10.1016/j.palaeo.2010.02.036.

Thibault, N., Husson, D., 2016. Climatic fluctuations and sea-surface water circulation patterns at the end of the Cretaceous era: calcareous nannofossil evidence. Palaeogeogr. Palaeoclimatol. Palaeoecol. 441:152–164. http://dx.doi.org/10.1016/j.palaeo.2015.07.049.

Thompson, G., Bryan, W.B., Frey, F.A., Sung, A.C., 1974. Petrology and geochemistry of basalts and related rocks from sites 214, 215, 217 DSDP Leg 22, Indian Ocean. In: von der Borch, C.C., Slater, J.G., et al. (Eds.), Initial Reports of the Deep Sea Drilling Project, 22. U.S. Government Printing Office, Washington:pp. 459–468 http://dx.doi.org/10.2973/dsdp.proc.22.119.1974.

Thunell, R.C., 1976. Optimum indices of calcium carbonate dissolution, in deep-sea sediments. Geology 4 (9):525–528. http://dx.doi.org/10.1130/0091-7613(1976)4<525:OIOCCD>2.0.CO;2.

Tobin, T.S., Ward, P.D., Steig, E.J., Olivero, E.B., Hilburn, I.A., Mitchell, R.N., Diamond, M.R., Raub, T.D., Kirschvink, J.L., 2012. Extinction patterns, δ^{18}O trends, and magnetostratigraphy from a southern high-latitude Cretaceous–Paleogene section: links with Deccan volcanism. Palaeogeogr. Palaeoclimatol. Palaeoecol. 350-352: 180–188. http://dx.doi.org/10.1016/j.palaeo.2012.06.029.

Tsujita, C.J., 2001. The significance of multiple causes and coincidence in the geological record: from clam clusters to Cretaceous catastrophe. Can. J. Earth Sci. 38 (2):271–292. http://dx.doi.org/10.1139/e00-048.

Vellekoop, J., Sluijs, A., Smit, J., Schouten, S., Weijers, J.W., Damsté, J.S.S., Brinkhuis, H., 2014. Rapid short-term cooling following the Chicxulub impact at the Cretaceous–Paleogene boundary. Proc. Natl. Acad. Sci. 111 (21):7537–7541. http://dx.doi.org/10.1073/pnas.1319253111.

Vermeij, G.J., 1995. Economics, volcanoes, and Phanerozoic revolutions. Paleobiology 21 (02):125–152. http://dx.doi.org/10.1017/S0094837300013178.

Vincent, E., Berger, W.H., 1985. Carbon dioxide and polar cooling in the Miocene: the Monterey hypothesis. In: Sundquist, E.T., Broecker, W.S. (Eds.), The Carbon Cycle and Atmospheric CO: Natural Variations Archean to Present. American Geophysical Union, Washington, D.C.:pp. 455–468 http://dx.doi.org/10.1029/GM032p0455.

Von der Borch, C.C., Sclater, J.G., Gartner Jr., S., Hekinian, R., Johnson, D.A., McGowran, B., Pimm, A.C., Thompson, R.W., Veevers, J.J., Waterman, L.S., 1974. Site 217. Initial Reports of the Deep Sea Drilling Project, 22. U.S. Government Printing Office, Washington:pp. 267–324 http://dx.doi.org/10.2973/dsdp.proc.22.108.1974.

Wignall, P.B., 2001. Large igneous provinces and mass extinctions. Earth Sci. Rev. 53 (1–2):1–33. http://dx.doi.org/10.1016/S0012-8252(00)00037-4.

Wilf, P., Johnson, K.R., Huber, B.T., 2003. Correlated terrestrial and marine evidence for global climate changes before mass extinction at the Cretaceous-Paleogene boundary. Proc. Natl. Acad. Sci. U. S. A. 100 (2):599–604. http://dx.doi.org/10.1073/pnas.0234701100.

Williams, D.F., Healy-Williams, N., Laschak, P., 1985. Dissolution and water-mass patterns in the southeast Indian Ocean, part I: evidence from recent to late Holocene foraminiferal assemblages. Geol. Soc. Am. Bull. 96 (2):176–189. http://dx.doi.org/10.1130/0016-7606(1985)96<176:DAWPIT>2.0.CO;2.

Zachos, J.C., Arthur, M.A., Dean, W.E., 1989. Geochemical evidence for suppression of pe-lagic marine productivity at the Cretaceous/Tertiary boundary. Nature 337, 61–64.

Zachos, J.C., Lohmann, K.C., Walker, J.C., Wise, S.W., 1993. Abrupt climate change and transient climates during the Paleogene: a marine perspective. J. Geol. 101 (2), 191–213.

Zepeda, M.A., 1998. Planktonic foraminiferal diversity, equitability and biostratigraphy of the uppermost Campanian-Maastrichtian, ODP leg 122, hole 762C, Exmouth Plateau, NW Australia, eastern Indian ocean. Cretac. Res. 19 (2):117–152. http://dx.doi.org/10.1006/cres.1997.0097.